Addis Ababa University

School Of Graduate Studies

Effect of Change of Contact Ratio on Contact Fatigue Stress of Spur Gears

A thesis submitted to the school of Graduate studies of Addis Ababa University in partial fulfillment of the Degree of Masters of Science in Mechanical Engineering (Mechanical Design Stream)

By
Michael G/mariam

Advisor
Dr. Daniel Tilahun

February, 2013
Addis Ababa

Acknowledgement

I would like to express my sincere appreciation and gratitude to Dr. Daniel Tilahun for being my advisor and for his valuable guidance, help and encouragement during the process of this thesis. Without his guidance and support this work would have been impossible. He was the one who inspire and encourage me to work on this project. His supervision, advice, guidance and encouragement have helped me tremendously, even when I thought I have failed to progress, stand again and finish my study.

I am also grateful to thank all staffs of Mechanical Engineering Department of EiT Especially Mr. Sirak A. for the cooperation in all matters as well as readiness and open mind for my enquiries.

My deepest appreciation is extended to my parents whose love and support has among other things helped me to achieve my goals as a student so far. I would like to thank my cousin Gezae W/gebriel and Muzit Goitom, and the rest of my family, for their fellowship and encouragement throughout my studies. In addition, I am grateful to my friends Kidanemariam G/Michael, Daniel Delibe, H/mariam Abriha, Temesgen Mathios, Simon Wodajo, Gidey G/yohannis(weizerit), and my fellow graduate students who have made the time spent at AAiT interesting and rewarding.

Abstract

The present research work dealt on the effect of change of contact ratio on the contact fatigue stresses generated on meshing spur gear teeth during power transmission. In the study different cases of six contact ratio gearing between 1.6 and 2.0 have been analyzed. For the different contact ratios considered the rate of load sharing and angular and radial position of load were determined on the involute profile of meshing tooth of each gearing. In addition to that the different stress conditions of this tooth for critical position (at the instant when the generated contact stress is at the maximum state) are determined. To come up at the result CATIA and Solid Works software involute spur gear models have been applied for stress analysis on ANSYS Workbench (FEM). From this study it is clear that, the higher contact ratio resulted in the higher generated tooth fatigue contact stresses life (i.e. the highest load carrying capacity). This is because of the decrease in value, and the change in location and direction of load applied on tooth involute in mesh to transmit power. At last the results obtained from ANSYS WB are compared with results of the AGMA gear formula results. They are comparable to each other.

Table of Contents

List of figures

List of tables

Nomenclature

b	Half of contact width
C_p	Elastic coefficient
C_a	Application factor for pitting resistance
C_s	Size factor for pitting resistance
C_m	Load distribution factor for pitting resistance
C_f	Surface condition factor
C_v	Dynamic factor for pitting resistance
S_c	Allowable contact stress
C_H	Hardness ratio factors for pitting resistance
CR	Contact ratio
D_p	Pinion pitch diameters,
D_g	Gear pitch diameters
E_e	Equivalent modulus of material
E_i	Young's Modulus for material i
F	Force acting over contact length
F	Face width
I	Geometry factor for pitting resistance
K_V	Dynamic factor
K_T	Temperature factors
K_R	Reliability factors
K_a	Application factor
K_H	Load distribution factor
$K_{H\beta}$	Face load distribution factor for contact stress
$K_{H\alpha}$	Transverse load distribution factor
L	Contact length
m	Module
P_{Max}	Maximum contact pressure
r_{ap}	Addendum circle radius of pinion
r_{ag}	Addendum circle radius of gear
r_{bp}	Base radius of pinion
r_{bg}	Base radius of gear
R_1	Radius of cylinder 1
R_2	Radius of cylinder 2
R_e	Equivalent radius of curvature
R_g	Radius of gear

R_p	Radius of pinion
S_c	Contact stress number
S_H	AGMA factor of safety, a stress ratio
T_p	Torque on pinion
ν_i	Poison ratio for material i
W_t	Transmitted tangential load
W_N	Normal force applied on pinion
W_t	Tangential component of force
Y_a	Addendum factor
Z_E	Elasticity factor
Z_l	Geometry factor for pitting resistance
Z_N	Stress cycle life factor
Z_R	Surface condition factor for pitting resistance
Z_V	Speed factor
μ	Coefficient of friction
σ_c	Contact stress
σ_{HO}	Nominal contact stress at pitch point
σ_{HP}	Permissible contact stress
σ_{Ort}	Maximum orthogonal shear stress
σ_{Von}	Maximum Von Miss Stress
σ_x	Shear stress along x
σ_y	Shear stress along y
σ_z	Shear stress along z
τ_{Max}	Maximum shear stress
	Pressure angle

CHAPTER ONE

1 INTRODUCTION

The motion from one shaft to another shaft may be transmitted with belts, ropes and chains. These methods are mostly used when the two shafts are having long center distance. But if the distance between the two shafts is very small, then gears are used to transmit motion from one shaft to another. In case of belts and ropes, the drive is not positive. There is slip and creep that reduces velocity ratio. But gear drive is a positive and smooth drive, which transmit velocity ratio. Gears are used in many fields and under a wide range of conditions such as in smaller watches and instruments to the heaviest and most powerful machineries like lifting cranes. Gears are most commonly used for power transmission in all the modern devices. These toothed wheels are used to change the speed or power between two stages (input and output). [B.Venkatesh et al., 2010]

Although gears have gained wide range of acceptance in all kinds of applications they have to resist the bending and fatigue stresses produced due to the cyclic load during power transmission. However; After the investigation of shot-peening to increase the tooth bending strength in gears, surface durability, in the form of macro and micro-pitting, is now considered the dominant restriction on gear life and performance. [Suzuki Y., 2004], has shown this, as it is depicted in figure 1.1.

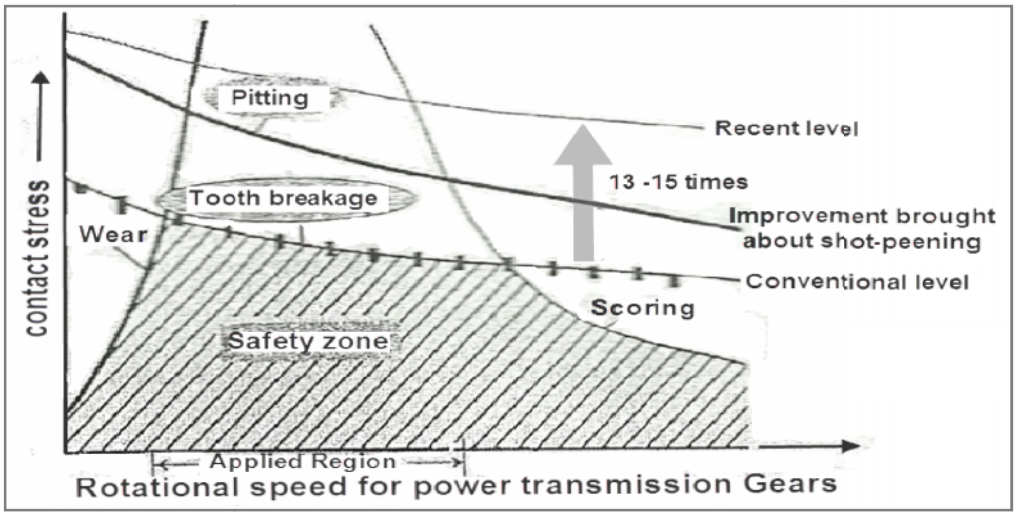

Figure 1.1: Failure of gears with respect to contact stress and rotational speed

In addition to that, failure of tooth due to bending (breakage) tends to be catastrophic to a gear unit, so the designer usually makes the teeth large enough so that they are definitely less appropriate to fail in

breakage mode than in a pitting mode. This makes the design life of a gear unit primarily dependent on its surface fatigue capacity (pitting resistance) rather than on its cantilever beam capacity (capacity to resist tooth breakage) [Solomon T, 2011]. So, theoretical analysis has to be carried out in the design stage of gears to prevent catastrophic failure during the power transmission period. Analyses in the past were performed using analytical methods, which required a number of assumptions and simplifications. In general, gear analyses are multidisciplinary, including calculations related to the tooth stresses and to tribological failures such as like wear or scoring [Zeping Wei, 2004] and pitting, the surface fatigue failure resulting from repetitions of high contact stress [Ali Raad H.,2009].

A majority of the heavily loaded transmissions used in military applications use gears with a contact ratio less than 2.0. The contact ratios of these transmissions are in the range of 1.3 to 1.8. So, the number of teeth in engagement at any instant is either one or two [M. Rameshkumar et al., 2010]. Many gear designs use increased pressure angle for increasing the load carrying capacity of gears with fixed module and center distance, but the contact ratio decreases. Tooth dynamic loads and noise increase due to decreased pressure angle. Hence increasing the load carrying capacity of gears for the above conditions can be done by the design of gears with a contact ratio greater than equal to 2.0. High contact ratio gears having a contact ratio greater than 2.0 have load sharing between two or three teeth during engagement and fewer loads per tooth [Elkholy,A.H., 1985].

1.1 Objective

The general objective of this thesis is to analyze effect of change of contact ratio on contact fatigue stress of involute spur gear tooth using the finite element method. And the specific objectives are:

- Modeling of the gear teeth using CATIA and Solid Works software which are powerful in gear teeth generation and modeling.
- The finite element analysis using ANSYS software considering different contact ratios to get the fatigue stresses of each condition. ANSYS is finite element structured software, and powerful and accurate in solving mechanical engineering problems.
- Finite element results are compared with analytical results.

1.2 Outline

This thesis is organized in to six chapters. In the first chapter introduction and justification of this thesis work and the objectives to be achieved are discussed. In chapter two, a review of literature relevant to this thesis work, which has been investigated by different researchers, is given. Chapter three is about contact mechanics, and how to use Hertz contact theory and AGMA relations in contact fatigue stress analysis in gears. In addition mechanism of creating contact ratio and teeth load sharing of spur gear teeth is studied. In chapter four, analytical and numerical method is used, to develop involutes spur gear using CATIA, and 3D finite element analysis mechanisms and steps of ANSYS workbench are discussed. In Chapter five the results and discussion of the study are presented. The conditions of fatigue stress and fatigue life with respect contact ratio variation is discussed. Finally, chapter six discuses conclusion of this thesis work.

CHAPTER TWO

2 LITERATURE REVIEW

The motion from one shaft to another shaft may be transmitted with belts, ropes and chains. These methods are mostly used when the two shafts are having long center distance. But if the distance between the two shafts is very small, then gears are used to transmit motion from one shaft to another. In case of belts and ropes, the drive is not positive. There is slip and creep that reduces velocity ratio. But gear drive is a positive and smooth drive, which transmit velocity ratio. Gears are used in many fields and under a wide range of conditions such as in smaller watches and instruments to the heaviest and most powerful machineries like lifting cranes. Gears are most commonly used for power transmission in all the modern devices. These toothed wheels are used to change the speed or power between two stages (input and output) [B.Venkatesh et al., 2010].

Although gears have gained wide range of acceptance in all kinds of applications they have to resist the bending and fatigue stresses produced due to the cyclic load during power transmission to prevent catastrophic failure of teeth. So, theoretical analysis has to be carried out in the design stage of gears to prevent catastrophic failure during the power transmission period. Analyses in the past were performed using analytical methods, which require a number of assumptions and simplifications. In general, gear analyses are multidisciplinary, including calculations related to the tooth stresses and to tribological failures such as like wear or scoring [Zeping Wei, 2004] and pitting, the surface fatigue failure resulting from repetitions of high contact stress[Ali Raad H.,2009]. From the many gear types different researches has studied on spur gear teeth surface contact stress.

[B.Venkatesh, 2010] has studied on helical gear which offers high contact and more friction and avoids slippage when compared to spur gear. To estimate the bending stress, three dimensional solid models for different number of teeth are generated by CATIA that is powerful and modern modeling software and the numerical solution is done by ANSYS, which is a finite element analysis package. His analytical investigation is based on Lewis stress formula. The aim of the

study is to focus on reduction of weight and thereby reducing the unbalance forces setup in the system.

[Ali Raad Hassan, 2009], Investigated natural frequencies and dynamic response of a spur gear sector using a two dimensional finite element model that offers significant advantages for dynamic gear analyses. The gear teeth are analyzed for different operating speeds. A primary feature of this modeling is determination of mesh forces using a detailed contact analysis for each time step as the gears roll through the mesh. ANSYS software has been used on the proposed model to find the natural frequencies and displacements and dynamic stresses by transient mode super position method. The effect of rotational speed of the gear on the dynamic response of gear tooth has been studied and design limits have been discussed on this study.

[Andrew Sommer, et al.], Demonstrated the early transient dynamic loading on teeth within a fixed-axis gear transmission arising from backlash and geometric manufacturing errors by utilizing a non-linear multi-body dynamics software model. Selection of the non-linear contact parameters such as the stiffness, force exponent, damping, and friction coefficients are presented for a practical transmission. Backlash between gear teeth which is essential to provide better lubrication on tooth surfaces and to eliminate interference is included as a defect and a necessary part of transmission design. Tensional vibration is shown to cause teeth separation and double-sided impacts in unloaded and lightly loaded gearing drives. Vibration and impact force distinctions between backlash and combinations of transmission errors are demonstrated under different initial velocities and load conditions. Additionally, the loading dynamics of a crank-slider mechanism with two-stage gear driving train is analyzed. The backlash and manufacturing errors in the first stage of the gear train are distinct from those of the second stage. By analyzing the signal at a location between the two stages, the mutually affected impact forces are observed from different gear pairs, a phenomenon not observed from single pair of gears.

[Evgeny Podzharov, et al., 2008] Studied in high precision and heavily loaded spur gears. In this study the effect of gear errors is negligible, so the periodic variation of tooth stiffness is the principal cause of noise and vibration. High contact ratio spur gears could be used to exclude or

reduce the variation of tooth stiffness. The analysis of static and dynamic transmission error of spur gears cut with standard tools of 20° profile angle is presented in this paper. A simple method to design spur gears with a contact ratio nearly 2.0 is used. It consists of increasing the number of teeth on mating gears and simultaneously introducing negative profile shift in order to provide the same center distance. Computer programs to calculate static and dynamic transmission error of gears under load have been developed. The analysis of gears using these programs showed that gears with high contact ratio have much less static and dynamic transmission error than standard gears.

[M. Rameshkumar, et al., 2010] Says the gears used in vehicles should have lesser noise and vibration. Even though helical gears will meet the requirement, they are prone for additional axial thrust problem. In his study high contact ratio (HCR) is one such gearing concept used for achieving high load carrying capacity with less volume and weight. Contact ratio greater than 2.0 in HCR gearing results in lower bending and contact stresses. This paper deals with finite element analysis of HCR, normal contact ratio (NCR) gears with same module, center distance and the comparison of bending, contact stress for both HCR, NCR gears. A two dimensional deformable body contact model of HCR and NCR gears is analyzed in ANSYS software. ANSYS Parametric Design language (APDL) is used for studying the bending and contact stress variation on complete mesh cycle of the gear pair for identical load conditions. The study involves design, modeling, meshing and post processing of HCR and NCR gears using single window modeling concept to avoid contact convergence and related numerical problems.

[P.J.L. Fernandes, et al., 1997] referred that surface contact fatigue is the most common cause of gear failure. It results in damage to contacting surfaces which can significantly reduce the load-carrying of components, and may ultimately lead to complete failure of a gear. The types of contact fatigue damage are discussed, and a number of actual examples are presented to illustrate this failure mode in practice in his study.

[Robert Basan, et al., 2008] Pitting of gears teeth flanks is one of the most pronounced type of damage that occurs in gears. Although it can manifest itself in a number of different forms, it is direct consequence of highly concentrated cyclic stresses and strains which develop in tooth

flank material during the mesh in conditions of simultaneous rolling and sliding contact. Due to such rather complex state of stress and strain that changes during the mesh, identification of critical locations in regard to fatigue damage and crack initiation is difficult task and requires detailed numerical analysis. For the determination of mentioned stresses and strains and their evolution during the mesh, a numerical model gear pair in mesh was developed and complete analysis procedure defined.

[Rubén D. Chacón, et al., 2005] In this paper a study of the stresses in the contact zone among a couple of spur gears is realized using the finite elements method. The analysis is done by using a plane model involving the contact between two teeth. The geometry is defined according to the standards of the American Gear Manufacturers Association (AGMA). The results obtained are compared with the value given by two others approaches. The first is the theory of Hertz when it is applied to two curved segments in contact. The second approach is the AGMA procedure for calculating contact stresses in spur gear. The results obtained are very similar either using FEM and Hertz´s theory. The contact pressure obtained by FEM is lower than the one obtained by means of Hertz´s theory, this fact reflects the influence of the geometry profile which allows the occurrence of contact zones with greater area, and therefore lower pressures.

[Sabah M.J.Ali, et al., 2007] concentrates on the effect of contact ratio change on the stresses generated on meshing gear teeth. Many cases of contact ratio (1.6, 1.7, 1.8, 1.9 & 2.0) have been studied. In each case the value and location of load were determined on the involute profile of meshing tooth. Also the angular position of this tooth for critical loading condition (at the instant when the generated root stresses at the maximum state) is analyzed. (ANSYS) programming using F.E.M have been applied for stress analysis on gear model. From this study it is clear that, the highest contact ratio resulted in the lowest generated tooth stresses (i.e. the highest load carrying capacity). This depends on the value, location and direction of load applied on tooth involute.

[Shreyash Patel, 2010] Developing an analytical approach and modeling procedure to evaluate stress distribution under velocity and moment would provide a useful tool to improve spur gear design with high efficiency & low cost. The purpose of this work is to analyze and validate the

stress distribution in spur & helical gears using contemporary commercial FEM program ANSYS coupled with the Pro/E solid modeler. Gear profiles are created in Pro Engineer using the Relation and Equation modeling procedure so as to make it a general model, dependant on certain key features like number of teeth, diametral pitch, and pressure and helix angle. These models were then analyzed for 3-D and 2-D bending stresses. Calculated results obtained when compared to standard AGMA stresses show good agreement.

[Sorin Cănănău, 2003] Performed on non-conforming elastic bodies in contact, whose deformation remains sufficiently small for the linear small strain theory of elasticity to be applicable, are in 3D contact over a line (or lines), named "contact line". Based on an exact geometry design of the involute gear tooth, a set of profile gears is obtained in order to calculate the 2D contact. A stress analysis was performed for CAD profiles results using the finite element procedure. The paper investigates the 2D analysis versus 3D analysis for stress in the root region of teeth. By this approach, is also investigated the influence of non-uniform load along contact line to the fillet stress.

[Tuan Nguyen, 2011] has presented procedures for compact design of non-standard spur gear sets with the objective of minimizing the gear size. The procedures are for long and short addendum system gear pairs that have an equal but opposite amount of hob cutter offset applied to the pinion and gear in order to maintain the standard center distance. Hob offset has shown to be an effective way to balance the dynamic tooth stress of the pinion and the gear to increase load capacity. The allowable tooth stress and dynamic response are incorporated in the process to obtain a feasible design region. Various dynamic rating factors were investigated and evaluated. The constraints of contact stress limits and involute interference combined with the tooth bending strength provide the main criteria for this investigation. A three-dimensional design space involving the gear size, diametral pitch, and operating speed was developed to illustrate the optimal design of the non-standard spur gear pairs.

[Zeping Wei, 2004] investigated the characteristics of an involute gear system including contact stresses, bending stresses, and the transmission errors of gears in mesh. To estimate transmission error in a gear system, the characteristics of involute spur gears were analyzed by

using the finite element method. The contact stresses were examined using 2-D FEM models. The bending stresses in the tooth root were examined using a 3-D FEM model. Current methods of calculating gear contact stresses use Hertz's equations, which were originally derived for contact between two cylinders. To enable the investigation of contact problems with FEM, the stiffness relationship between the two contact areas is usually established through a spring placed between the two contacting areas. This can be achieved by inserting a contact element placed in between the two areas where contact occurs. The results of the two dimensional FEM analyses from ANSYS are presented. His thesis also considers the variations of the whole gear body stiffness arising from the gear body rotation due to bending deflection, shearing displacement and contact deformation. Many different positions within the meshing cycle were investigated.

[Ali Raad Hassan, 2009], Analyzed contact stress between two spur gear teeth considering different contact positions, for a represented a pair of mating gears during rotation. A programme has been developed to plot a pair of teeth in contact. This programme was run for each 3° of pinion rotation from the first location of contact to the last location of contact to produce 10 cases. Each case was represented a sequence position of contact between these two teeth. He used the programme to get graphic results for the profiles of these teeth in each position and location of contact during rotation. Finite element models were made for these cases and stress analysis was done. Finally the presented finite element analysis results were compared with theoretical calculations, wherever available.

[Solomon Tekeste, 2011] Come up to the two main factors that affect the service life of gears: surface durability and tooth bending strength. Pitting and scoring is a phenomenon in which small particles are removed from the surface of the tooth due to the high contact stresses that are present between mating teeth. After the investigation of shot pinning to increase the tooth bending strength in gears, surface durability, in the form of macro and micro-pitting, was considered as the dominant restriction on gear life and performance. The main objective of his thesis is to develop a method for the investigation of surface fatigue in involute spur gears using finite element analysis. In achieving this two dimensional & three dimensional equivalent

contacting cylinders to model involute spur gear in contact and three dimensional model of involute spur gear is used.

Modeling of involutes spur gear to study contact stress under different working conditions using CATIA & ANSYS software is done. In addition parametric study to investigate the effect of loading condition and material types in contact stress in gears, estimation of surface fatigue in rolling-sliding contact condition in spur gear by finite element method using ANSYS Workbench software, effect of initial surface roughness on surface fatigue is studied. The results obtained are compared with analytical method.

According to [Robert B. and et al., 2008] study Pitting of gears teeth flanks is one of the most pronounced types of damage that occurs in gears. Pitting is phenomenon in which small particles are removed from the surface of the tooth because of the high contact forces that are present between mating teeth. It is actually the fatigue failure of the tooth surface [J. Shigley, 2006]. Complex stresses within the contact zone cause surface and subsurface fatigue failures. The pits seen on the teeth grow in size and depth, ultimately resulting in tooth fracture and spalling. [Douglas Wright, 2005] Pitting occurs only after a large number of repeated loading on the contact surfaces of the teeth. It is found to occur most frequently at the pitch circle - where relative sliding of the teeth is zero and the hydrodynamic lubricant film tends to break down.

Pitting commonly appears on operating surfaces of gear teeth, a fundamental cause is excessive loading that raised contact stresses beyond critical levels. [Solomon T., 2011] has studied on the fatigue contact stress of involute spur gear teeth. On the study in hand the effect of the contact ratio on the contact stress has studied developing different models for the selected contact ratio of paired gear teeth. Contact ratio can be defined as a number of teeth in contact as these teeth pass through the contact zone [Solomon T., 2011]. The finite element method software, ANSYS is taken as a tool for the analysis after importing the developed spur gear teeth model in CATIA and Solid Works modeling software.

CHAPTER THREE

3 SPUR GEAR TOOTH THEORY- SURFACE FAILURE

3.1 Surface Failure Basic Concepts

When two bodies having curved surfaces are pressed together, point or line contact changes to area contact, and the stresses developed in the two bodies are three- dimensional. [R. L. Norton, 2006] When the two surfaces are in pure rolling contact, or are primarily rolling in combination with a small percentage of sliding, a different surface failure mechanism comes into play, called surface fatigue. Many applications of this condition exist in such as ball and roller bearings, cams with roller followers, nip rolls, and spur or helical gear tooth contact. All except the gear teeth and nip rolls typically have essentially pure rolling with only about I% sliding. Gear teeth have significant sliding at portions of their tooth interface and this will change the stress state significantly compared to the pure rolling cases. Typical failures are seen as cracks, pits, or flaking in the surface material.

The most general case of contact stress occurs when each contacting body has a double radius of curvature; that is, when the radius in the plane of rolling is different from the radius in a perpendicular plane, both planes are taken through the axis of the contacting force.

There are two kinds of stresses in gear teeth, root bending stresses and tooth contact stresses. These two stresses results in the failure of gear teeth, root bending stress results in fatigue fracture and contact stresses results in pitting failure at the contact surface. So both these stresses are to be considered when designing gears. Usually heavily loaded gears are made of ferrous materials that have infinite life for bending loads. But it is impossible to design gears with infinite life against surface failure. In this thesis the surface failure mode is studied based on the calculation of contact stresses.

Mating gear teeth have a combination of rolling and sliding at their interface. At the pitch point their relative motion is pure rolling. The percentage of sliding increases with distance from the pitch point. [R. L. Norton, 2006] an average value of 9% sliding is sometimes taken to represent the combined roll-slide motion between the teeth. The stresses at the tooth surface are dynamic Hertzian contact stresses in combined rolling and sliding. These stresses are three-dimensional and have peak values either at the surface or slightly below it, depending on the amount of sliding present in combination with rolling.

Depending on the surface velocity tooth radii of curvature and lubricant viscosity a condition of full or partial elastohydrodynamic (EHD) lubrication or of boundary lubrication may exist in the interface. If sufficient, clean lubricant of an appropriate type is provided in order to create at least partial EHD lubrication (specific film thickness A > 2) and prevent surface failure by the adhesive, abrasive, or corrosive mechanisms, then the ultimate failure mode will be pitting and spalling due to surface fatigue as shown figure (3.1).

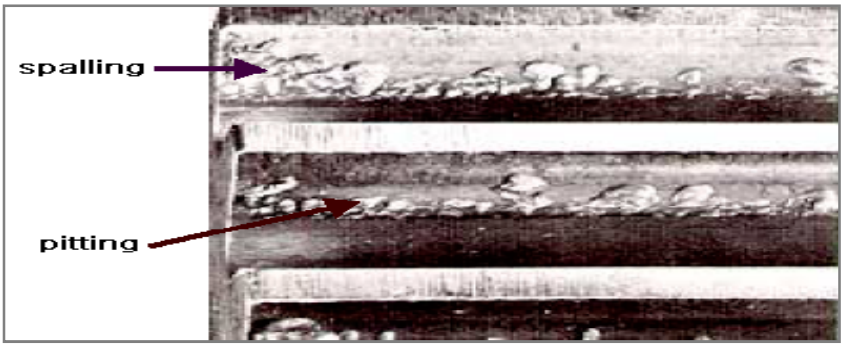

Figure 3.1: Pitting and spalling of gear teeth

Under contact conditions, gear teeth are subjected to Hertzian contact stresses and elasto-hydrodynamic lubrication. Excessive loading and lubrication breakdown can cause combinations of abrasion, pitting and scoring. We can define the surface failures as follows:

1. Abrasive wear: is caused by the presence of foreign particles, in gears that are not enclosed, in enclosed gears that were assembled with abrasive particles present, and in gears lubricated by an oil supply with inadequate filtration.

2. Scoring: occurs at high speeds when adequate lubrication is not provided by the elasto hydrodynamic action. Lack of lubrication causes high sliding friction. High tooth loading and high sliding velocities that produce a high rate of heat in the localized contact region causes welding and tearing of surfaces apart. Scoring can often be prevented by directing adequate flow of appropriate lubricant that maintains hydrodynamic lubrication. Surface finish is also an important factor for scoring.

3. Pitting or surface fatigue failure: Pitting is phenomenon in which small particles are removed from the surface of the tooth because of the high contact forces that are present between mating teeth. It is actually the fatigue failure of the tooth surface [J. Shigley, 2006]. Complex stresses within the contact

zone cause surface and subsurface fatigue failures. An example of pitch line contact fatigue is shown in figure (3.1) [T.E. Tallian, 2009]. The pits seen on the teeth grow in size and depth, ultimately resulting in tooth fracture and spalling. [Douglas Wright, 2005] Pitting occurs only after a large number of repeated loading on the contact surfaces of the teeth. It is found to occur most frequently at the pitch circle - where relative sliding of the teeth is zero and the hydrodynamic lubricant film tends to break down.

3.2 Hertz Theory of Contact

In many engineering applications, such as rolling bearings, gears, cams, etc., machine components whose functioning depends upon rolling and sliding motion in contact along surfaces while under load. In this case, the contacting surfaces are non-conformal, hence the resulting contact areas are very small and the pressures are very high. From the point of view of machine design it is essential to know the values of stresses acting in such contacts. These stresses can be determined, from the analytical formulae, based on the theory of elasticity, developed by Hertz in1881. [H. Hertz, et al., 1986]

The contact between two surfaces gives rise to an area of contact, and a pressure distribution over this contact area. If the surfaces have a simple geometry, the contact theory of Hertz (1881) can be used for calculating the contact area and the pressure distribution. The shape of the contact area depends on the shape (curvature) of the contacting bodies. For example, point contacts occur between two balls, line contacts occur between two parallel cylinders, and elliptical contacts, which are the most frequently found in many practical engineering applications, occur when two cylinders are crossed, or a moving ball is in contact with the inner ring of a bearing, or two gear teeth are in contact. To illustrate the contact between two elastic bodies, the simpler contact of two parallel cylinders Figure (3.2) is presented based on the Hertz theory. This type of contact is used to derive contact pressure distribution, stresses and displacements for the spur gear teeth in contact. [Vitor Manuel, 2005]

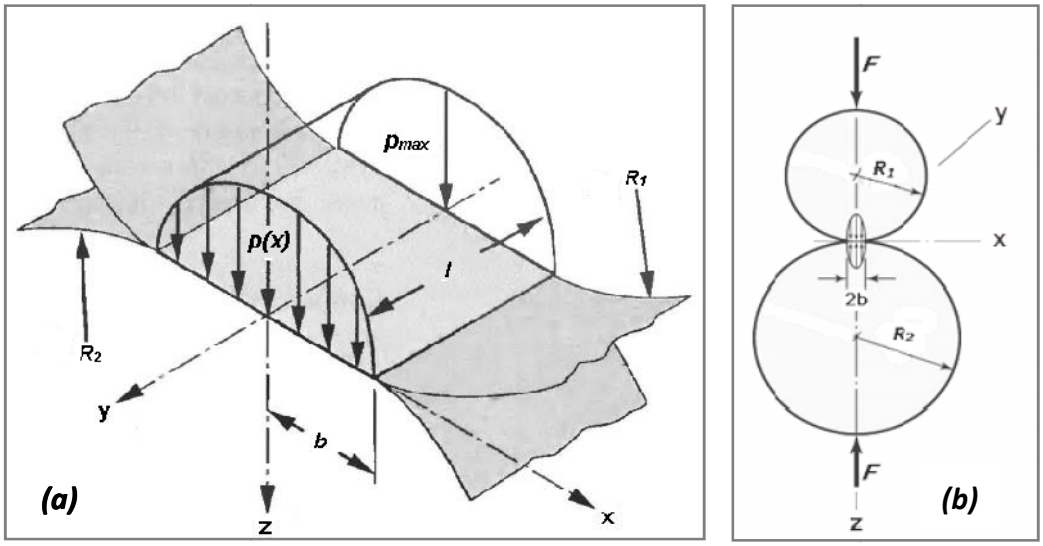

Figure 3.2: Ellipsoidal-prism pressure distribution in cylindrical contact: a. 3D view, b. 2D view

Where

- R1 is the radius of cylinder 1
- R2 is the radius of cylinder 2
- P(x) is the pressure distribution
- b is half of the contact width
- *l* is the contact length

When cylinders are in line contact, continued by a force F, a flattened rectangular zone exists in which the pressure distribution is elliptical. The pressure, P in between the cylinders will be:

$$p = \frac{2F}{\pi b^2 l}\sqrt{b^2 - x^2} \qquad 3.1$$

Where *F* is the force acting over the contact length l and 2b is the contact width. The maximum contact pressure at x = 0 (or at the line the force is applied) is

$$p_{max} = \frac{2F}{\pi b l} \qquad 3.2$$

$$b = \left\{\frac{4F}{\pi l}\frac{\left[\left(1-\boldsymbol{\nu}_1^2\right)/E_1\right] + \left[\left(1-\boldsymbol{\nu}_2^2\right)/E_2\right]}{(1/R_1) + (1/R_2)}\right\}^{1/2} \qquad 3.3$$

[Smith, et al., 1958] proposed analytical model for surface contact stress is used here. Taking axes $x, y,$ and z as the tangential, radial and axial directions at the contact point and assuming the plane strain case at the contact point, the stresses at xy plane can be written as,

$$\sigma_x = -\frac{p_{max}}{\pi}\left\{(b^2 + 2x^2 + 2y^2)\frac{y}{b}\bar{\varphi} - 2\pi\frac{y}{b} - 3xy\varphi + \mu\left|(2x^2 - b^2 - 3y^2)\varphi + 2\pi\frac{x}{b} + 2b2-x2-y2xb\varphi\right.\right. \quad 3.4$$

$$\sigma_y = -\frac{p_0}{\pi}y(b\bar{\varphi} + x\varphi + \mu y\varphi) \quad 3.5$$

$$\sigma_z = -\frac{2\nu}{\pi}p_{max}\left\{\left|(b^2 + x^2 + y^2)\frac{z}{b}\bar{\varphi} - \frac{\pi y}{b} - 2xy\varphi\right|\right.$$
$$+ \mu\left|(x^2 - b^2 - y^2)\varphi + \frac{\pi x}{b}\right.$$
$$\left.\left. + (b^2 - x^2 - y^2)xb\varphi\right|\right\} \quad 3.6$$

$$\tau_{xy} = -\frac{p_{max}}{\pi}\left\{y^2\varphi + \mu\left|(b^2 + 2x^2 + 2y^2)\frac{y}{b}\bar{\varphi}\right| - 2\pi\frac{y}{b} - 3xy\varphi\right\} \quad 3.7$$

Where p_{max} the maximum surface pressure, μ is the coefficient of friction, and b is the contact width, and φ and $\bar{\varphi}$ can be written as

$$\varphi = \frac{\pi}{\lambda_1}\frac{1 - \lambda_3}{\lambda_3\sqrt{2\lambda_{3+\lambda_4}}} \quad 3.8a$$

$$\bar{\varphi} = \frac{\pi}{\lambda_1}\frac{1 + \lambda_3}{\lambda_3\sqrt{2\lambda_{3+\lambda_4}}} \quad 3.8b$$

And λ_1, λ_2, λ_3 and λ_4 are given as

$$\lambda_1 = (b + x)^2 + y^2 \quad 3.9a$$

$$\lambda_2 = (b - x)^2 + y^2 \quad 3.9b$$

$$\lambda_3 = \left(\frac{\lambda_2}{\lambda_1}\right)^{1/2} \quad 3.9c$$

$$\lambda_4 = \frac{(\lambda_1 + \lambda_2 - 4b^2)}{\lambda_1} \quad 3.9d$$

Using the above equations the principal stresses and the maximum shear stress at y=0 can be calculated as follow. Along the y axis, the orthogonal stresses are,

$$\sigma_y = -\frac{p_{max}}{\sqrt{1+\left(\frac{y}{b}\right)^2}} \quad 3.10$$

$$\sigma_x = -p_{max}\left\{\left[2-\frac{1}{1+\left(\frac{y}{b}\right)^2}\right]\sqrt{1+\left(\frac{y}{b}\right)^2}-2\frac{y}{b}\right\} \quad 3.11$$

$$\sigma_z = -2p_{max}\left[\sqrt{1+\left(\frac{y}{b}\right)^2}\right]-\frac{y}{b} \quad 3.12$$

These equations are useful for rolling contact occurred between gear teeth. The largest principal stress is compressive and located at the center of the rectangular flat and is $-p_{max}$ in magnitude. The largest shear stress is approximately $0.30p_{max}$ and is located at about $0.78b$ below the surface. The maximum compressive stress is repeatedly applied in rolling cylinders. At a position of $y = 0.4b$, $z = 0.915b$ the shear stress has a magnitude of $0.25p_{max}$ but is completely reversed in rolling cylinders. The peak values of the equivalent stress using the Von Mises criterion, the maximum shear stress, and the maximum orthogonal shear stress can be calculated from the maximum Hertz stress as follows [Zeping Wei, 2004]:

$$Maximum\ shear\ stress, \quad \tau_{max} = 0.30p_{max} \quad 3.13$$

$$Maximum\ Von Mises\ stress, \quad \sigma_{von} = 0.57p_{max} \quad 3.14$$

$$Maximum\ orthogonal\ shear\ stress, \quad \sigma_{ort} = 0.25p_{max} \quad 3.15$$

3.3 Spur Gear – Buckingham Contact Stress Equation

Buckingham adapted the Hertz contact stress equation for a pair of gear teeth shown in Figure (3.3). He treated a pair of gear teeth as two cylinders of radii equal to the radii of curvature of the mating involutes at the pitch point. From basic involute geometry, these radii are given as equations (3.17). The way in which tooth surfaces of properly aligned gears make contact with each other is responsible for the heavy

loads that gears are able to carry. To obtain an expression for the surface-contact stress, the Hertz theory is employed.

It has already noted that the first evidence of wear occurs near the pitch line. The radius of curvature of the tooth profile has an effect on the amount of deformation and on the width of the resulting contact bands.

As it is discussed previously, meshed spur gears can be modeled by two parallel cylinders in contact. From equation (3.3), half of the contact width b, can be rewritten as,

$$b = \sqrt{\frac{4FR_e}{\pi l E_e}} \qquad 3.16$$

Where, R_e is the equivalent radius of curvature, given by

$$R_e = \frac{1}{\left({}^{1}/_{R_1} + {}^{1}/_{R_2}\right)} \qquad 3.17$$

Where R_1 and R_2 are the instantaneous values of the radii of curvature on the pinion- and gear-tooth profiles, respectively, at the point of contact.

At the pitch point $R_1 = R_P$ and $R_2 = R_G$ and given by

$$R_P = \frac{D_P sin\phi}{2} \quad and \; R_G = \frac{D_G sin\phi}{2} \qquad 3.18$$

Where D_P & D_G are the pitch diameters of Pinion and gear respectively, and ϕ is the pressure angle. Therefore, at the pitch point R_e becomes

$$R_e = \frac{1}{\frac{2}{sin\phi}\left({}^{1}/_{D_P} + {}^{1}/_{D_G}\right)} \qquad 3.19$$

And E_e is the equivalent modulus of elasticity of the material,

$$E_e = \frac{1}{[(1-\boldsymbol{\nu_1^2})/E_1] + [(1-\boldsymbol{\nu_2^2})/E_2]} \quad 3.20$$

Substitute the value of b from equation (3.16) into (3.2), to find the maximum contact pressure, p_{max} results in

$$p_{max} = -\left[\frac{FE_e}{\pi l R_e}\right]^{1/2} \quad 3.21$$

For the driver pinion, and gear follower,

$$F = W_n = \frac{W_t}{cos\phi} = \frac{T_P}{R_P cos\phi} \quad 3.22$$

Where

- R_P is the radius of the pinion at the contact point and
- T_P is the torque on the pinion
- W_n the normal force applied on the pinion
- W_t tangential component of the normal force

Substitute the value of F from equation (3.22) into (3.21) results

$$p_{max} = \sigma_C = -\left[\frac{T_P E_e}{\pi l R_P cos\phi R_e}\right]^{1/2} \quad 3.23$$

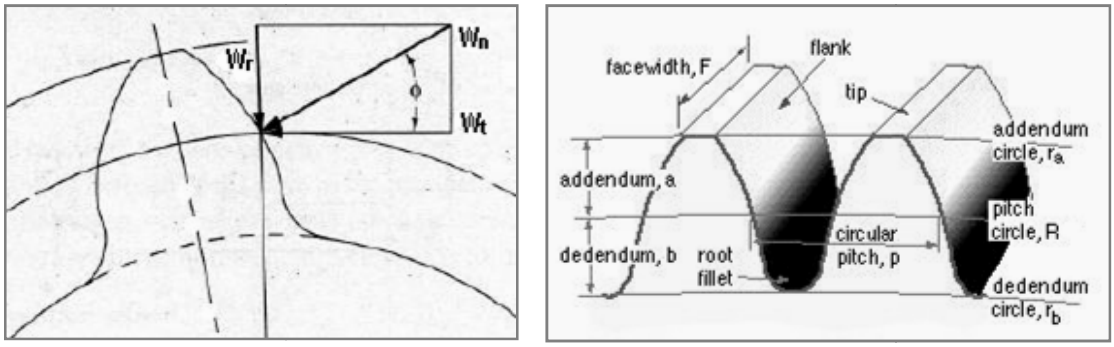

(a) (b)

Figure 3.3: Tooth load at the pitch surface element: (a) 2D, (b) 3D

And half-width b of gear is expressed as

$$b = \left\{ \frac{4W_t}{\pi F cos(\phi)} \frac{\left[(1-\boldsymbol{\nu_1^2})/E_1\right] + \left[(1-\boldsymbol{\nu_2^2})/E_2\right]}{(1/R_1) + (1/R_2)} \right\}^{1/2} \quad 3.24$$

Where ν_1, ν_2, E_1, and E_2 are the elastic constants and R_1 and R_2 are the radius of curvature of the two contacting gear teeth.

To adapt these relations to the notation used in gearing, we replaced force F by $W_t/cos\phi$, and l by the face width F. With these changes, we can substitute the value of b as given by Eq. (3.24). Replacing p_{max} by σ_C , the surface compressive stress (Hertzian stress) of the meshed gear teeth is found from the equation

$$\sigma_C^2 = \frac{W^t}{\pi F cos\phi} \frac{(1/R_1) + (1/R_2)}{\left[(1-\boldsymbol{\nu_1^2})/E_1\right] + \left[(1-\boldsymbol{\nu_2^2})/E_2\right]} \quad 3.25$$

Where σ_c is the contact stress

Pure rolling exists only at the pitch circle contact motion of spur gear teeth pair, elsewhere the motion is a mixture of rolling and sliding. Equation (3.23) does not account for any sliding action of contacting surfaces in the evaluation of stress. But in the case of sliding action note that AGMA uses $\boldsymbol{\mu}$ for Poisson's ratio instead of $\boldsymbol{\nu}$ as is used here.

Note: in Eq. (3.25), that the denominator of the second group of terms contains four elastic constants, two for the pinion and two for the gear. As a simple means of combining and tabulating the results for various combinations of pinion and gear materials, AGMA defines an elastic coefficient C_p by the equation below,

$$C_p = \left[\frac{1}{\pi\left(\frac{1-\nu_1^2}{E_1} + \frac{1-\nu_2^2}{E_2}\right)} \right]^{1/2} \quad 3.26$$

With this simplification, and the addition of a velocity factor K_v , Eq. (3.25) can be written as

$$\sigma_C = -C_p \left[\frac{K_v W^t}{F cos\phi} \left(\frac{1}{R_1} + \frac{1}{R_2} \right) \right]^{1/2} \quad 3.27$$

Where the sign is negative because σ_C is a compressive stress.

3.3.1 Spur Gear Tooth Contact Fatigue Analysis

Pitting is a fatigue failure where small cracks form in the tooth surface and then grow to the point where small, round bits of metal break out of the tooth surface. Traditionally, the gear designer first determines a pitch diameter and a face width for the pinion that are large enough for the pinion to last for the required service life with a probability of failure less than 1%. This determination is based on a possible pitting fatigue failure. It is assumed in the beginning that the surface finish, the tooth accuracy, the lubrication, and the needed profile and helix modifications will all be carried out well enough to avoid any serious risk of scuffing. Normally, the pinion is more appropriate to fail in pitting than the gear, so the sizing of the pinion tends to determine the needed size of the gear. After the pitch diameter of the pinion has been determined, the size of the teeth is determined by calculations regarding a possible failure in tooth breakage.

[Buckingham, 1969], conducted a number of tests relating the fatigue at 10^8 cycles to endurance strength (Hertzian contact pressure). While there is evidence of an endurance limit at about $3(10^7)$ cycles for cast materials, hardened steel rollers showed no endurance limit up to $4(10^8)$ cycles. Subsequent testing on hard steel shows no endurance limit. Hardened steel exhibits such high fatigue strengths that its use in resisting surface fatigue is wide spread. [Solomon T., 2011]

To determine the surface fatigue strength of mating materials, Buckingham designed a simple machine for testing a pair of contacting rolling surfaces, in connection with his investigation of the wear of gear teeth. Buckingham gathered large numbers of data from many tests so that considerable design information is now available. To make the results useful for designers, Buckingham defined a load-stress factor, also called a wear factor, which is derived from the Hertz equations. The maximum contact pressure, (p_{max}) and half width of the contact zone, (b) are defined in equations (3.2) and (3.3) respectively, for contacting cylinders.

If we then assign the length of the cylinders as F (for width of gear) instead of l and remove the square root sign, Eq. (3.24) becomes

$$b^2 = \frac{4W_t}{\pi F cos(\phi)} \frac{\left[(1-\boldsymbol{\nu}_1^2)/E_1\right] + \left[(1-\boldsymbol{\nu}_2^2)/E_2\right]}{(1/R_1) + (1/R_2)} \qquad 3.28$$

We can define a surface endurance strength S_C using equation (3.2) as

$$S_C = \frac{2W_n}{\pi bF} \tag{3.29}$$

which may also be called contact strength, the contact fatigue strength, or the Hertzian endurance strength. The strength is the contacting pressure which, after a specified number of cycles, will cause failure of the surface. Such failures are often called wear because they occur over a very long time. They should not be confused with abrasive wear, however. By squaring Eq. (3.16), substituting b^2 from Eq. (3.28), and rearranging, we obtain

$$\frac{W_n}{F}\left(\frac{1}{R_1 + R_2}\right) = \pi S_C^2 \left[\frac{(1 - \boldsymbol{\nu}_1^2)}{E_1}\right] + \left[\frac{(1 - \boldsymbol{\nu}_2^2)}{E_2}\right] = K_1 \tag{3.30}$$

The left expression consists of parameters a designer may seek to control independently. The central expression consists of material properties that come with the material and condition specification. The third expression is the parameter K_1, Buckingham's load stress factor, determined by a test fixture with values W_n, F, R_1, R_2 and the number of cycles associated with the first tangible evidence of fatigue. In gear studies a similar K factor is used:

$$K_G = \frac{K_1}{4} sin\varphi \tag{3.31}$$

Where φ is the tooth pressure angle, and the term $\left[\frac{(1-\boldsymbol{\nu}_1^2)}{E_1}\right] + \left[\frac{(1-\boldsymbol{\nu}_2^2)}{E_2}\right]$ is defined as $1/(\pi C_P^2)$, so that

$$S_C = C_P \sqrt{\frac{W_n}{F}\left(\frac{1}{R_1} + \frac{1}{R_2}\right)} \tag{3.32}$$

Equation (3.32) can be used in design to find an allowable surface stress by using a design factor. Since this equation is nonlinear in its stress-load transformation, the designer must decide if loss of function denotes inability to carry the load. If so, then to find the allowable stress, one divides the load W_n by the design factor nd:

$$S_C = C_P\sqrt{\frac{W_n}{Fn_d}\left(\frac{1}{R_1+R_2}\right)} = \frac{C_P}{\sqrt{n_d}}\sqrt{\frac{W_n}{F}\left(\frac{1}{R_1+R_2}\right)} = \frac{S_P}{\sqrt{n_d}} \quad 3.33$$

And $n_d = (S_C/\sigma_C)^2$. If the loss of function is focused on stress, then $n_d = S_C/\sigma_C$,

Buckingham and others reported K_1 for 10^8 cycles and nothing else. This gives only one point on the $S_C\, V_s\, N$ curve [J. Shigley, 2006]. For cast metals this may be sufficient, but for wrought steels, heat treated, some idea of the slope is useful in meeting design goals of other than 10^8 cycles.

Experiments show that $K1$ versus N, K_G versus N, and S_C versus N data are rectified by $log - log$ transformation. This suggests that

$$K_1 = \alpha_1 N^{\beta_1}$$

$$K_G = aN^b$$

$$S_C = \alpha N^{\beta}$$

The three exponents are given by

$$\beta_1 = \frac{\log(K_1/K_2)}{\log(N_1/N_2)}$$

$$b = \frac{\log(K_{G1}/K_{G2})}{\log(N_1/N_2)}$$

$$\beta = \frac{\log(S_{C1}/S_{C2})}{\log(N_1/N_2)}$$

For applications where little or no pitting is permissible, the American Gear Manufacturers Association ($AGMA$) uses $\beta = -0.056$ between $10^4 < N < 10^{10}$ if the designer has no data to the contrary beyond 10^7 cycles.

$AGMA$ Standard, [$ANSI/AGMA$, 2001] suggests allowable contact-stress numbers (for 10^7 cycles and 0.99 reliability for through hardened steel gears) as high as

$$(S_C)_{10^7} = 2.22H_B + 200MPa \quad 3.34$$

For grade 1

$$(S_C)_{10^7} = 2.41H_B + 237MPa \quad 3.35$$

And for grade 2 steel

AGMA Standard 2101-D04 strength equation, for allowable contact stress, σ_{HP} is given by

$$\sigma_{HP} = \frac{S_C Z_N C_H}{S_H K_T K_R} \quad 3.36$$

Where,

- σ_{HP} is Permissible contact stress taking into account fatigue strength, [MPa]
- S_c is Fatigue limit taking into account contact stress, [MPa]
- Z_N is stress cycle factor for pitting resistance
- C_H is the hardness ratio factors for pitting resistance
- K_T is the temperature factor
- K_R is the reliability factor
- S_H is the AGMA factor of safety, a stress ratio

3.3.2 Pitting Resistance Stress Cycle Factor Analysis

As discussed earlier the actual cylindrical gear-tooth rating formulae for pitting resistance are based on Hertz's results for the calculation of contact pressure between two curved surfaces. They have also been improved with modifications in the new standards to consider load sharing between adjacent teeth, the load increment due to external and internal dynamic loads, uneven distribution of load over the face width due to mesh misalignment caused by inaccuracies in manufacture, and elastic deformations, etc [G. G. Reyusing, et al., 2007].

Based on that AGMA Standard 2101-D04 provides the following rating formula and permissible stresses applicable for calculating the pitting resistance of external cylindrical involute gear teeth operating on parallel axes.

$$\sigma_C = C_p \sqrt{\frac{W^t . K_O . K_V . K_H . K_S . Z_R}{F . d_P . Z_I}} \leq \sigma_{HP} = \frac{S_C Z_N C_H}{S_H K_T K_R} \quad 3.37$$

Where:

- σ_C: Pitting resistance (Contact stress), [MPa]
- C_p: Elastic coefficient, $[\sqrt{Mpa}]$
- W^t: Transmitted tangential load, [N]

- K_O: Overload factor
- K_V: Dynamic factor
- K_H: Load distribution factor
- K_S: Size factor
- Z_R: Surface condition factor for pitting resistance
- F: Facewidth, [mm]
- d_P: Operating diameter of pinion, [mm]
- Z_I: Geometry factor for pitting resistance

By means of mathematical processing of formula (3.37) it is possible to determine the stress cycle factor for pitting resistance according to equation (3.38).

$$Z_N = C_p \cdot \sqrt{\frac{W^t . K_O . K_V . K_H . K_S . Z_R}{F . d_P . Z_I}} \cdot \frac{S_H . K_T . K_R}{S_c . C_H} \qquad 3.38$$

3.3.3 Factor of Safety for Pitting Strength analysis

The ANSI/AGMA standards 2101-D04 contains a safety factor S_H guarding against pitting failure. The definition of S_H from equation (3.37)

$$S_H = \frac{S_C Z_N C_H / (K_T K_R)}{\sigma_C} = \frac{\text{fully corrected contact strength}}{\text{contact stress}} \qquad 3.39$$

3.3.4 Determination of the Expected Fatigue Lifetime

Knowing the interrelation of factor Z_N with the fatigue limit stress equivalent to a certain number of load cycles, it is possible to determine the useful expected fatigue lifetime in the condition of contact stress in the teeth with corresponding permissible stress for failure [G. G. Reyusing, et al., 2007]. Under these conditions, the number of load cycles expected by pitting (n_{Lh}) can be evaluated with the stress cycle factor Z_N determined by the formulas (3.38) and graphical information presented on AGMA 2101-D04. Once certain that the numbers of load cycles corresponding to calculated values of factor Z_N the hours of expected fatigue lifetime ($H_{\sigma H}$) can be known by means of the following equation.

$$H_{\sigma H} = \frac{n_{Lh}}{60 . n . q} [\text{hours}] \qquad 3.40a$$

But $n_{Lh} = \left(\frac{Z_N}{2.466}\right)^{-\left(\frac{1}{0.058}\right)}$ 3.40b

Where:

n_{Lh}: Number of load cycles expected by pitting in corresponding with stress cycle factor Z_N
n: Rotational speed, (min^{-1})
q: Number of load application by 1 turn of gear

3.3.5 Contact Fatigue Criterion

Rolling contact fatigue is based on the Lundberg-Palmgren theory [G. Lundberg, et al., 1946]. The Lundberg-Palmgren theory postulates that the stress responsible for fatigue damage is the orthogonal shear stress, which can be derived from the Hertzian pressure distribution in the contact surface and the subsurface. The orthogonal shear stress amplitude reaches a maximum simultaneously in two planes, one parallel and one perpendicular to the contact surface. Damage resulting from contact stresses starts as a localized, inelastic cyclic deformation (localized yielding or distortion) followed by the initiation and propagation of a crack. Inelastic deformation theories are based on material deformation occurring when either the maximum shearing stress (Tresca's criterion) or the maximum octahedral shearing stress (von Mises criterion) at any point in a component reaches a critical value that causes slip of the crystal along specific crystallographic planes [A.P. Boresi, et al., 1985]. The maximum shearing stress is given by:

$$\tau_{max} = \frac{1}{2}(\sigma_1 - \sigma_3)$$

Where σ_1 and σ_3 are the maximum and minimum values of the principal stresses at a point. The maximum octahedral shearing stress is given by the equation:

$$\tau_{oct} = \frac{1}{3}\sqrt{(\sigma_1 - \sigma_2)^2 + (\sigma_2 - \sigma_3)^2 + (\sigma_3 - \sigma_1)^2}$$

Where σ_1 and σ_3 are defined as before and σ_2 is the third principal stress. If normal forces act alone that is the friction coefficient is zero, the stresses would be [K. C. Ludema, 1983]:

$$\sigma_{1MAX} = -p_{max}, \sigma_{2MAX} = p_{max}, and\ \sigma_{3MAX} = -0.5p_{max}$$

Maximum shear stress, $\tau_{max} = 0.3p_{max}$

Maximum octahedral shear stress, $\tau_{oct(max)} = 0.27 p_{max}$

and these values of τ_{max} and $\tau_{oct(max)}$ occur on the y-axis at a certain distance below the contact surface. This distance is a function of only contact geometry.

3.4 Contact Ratio

Contact ratio is defined as a number of teeth in contact at one time as these teeth pass through the contact zone. In other words, contact ratio is a number which indicates the average number of pairs in contact. It is impractical to make C.R less than unity. [Robert L. Norton, 2006] If the contact ratio is one, then one pair of teeth leaves contact just as the next pair begins contact. This is undesirable, because slight errors in the tooth spacing will cause oscillations in the velocity, vibration, and noise. In addition, the load will be applied at the tip of the tooth, creating the largest possible bending moment. At larger contact ratios than 1, there is the possibility of load sharing among the teeth. For contact ratios between 1 and 2, which are common for spur gears, there will still be times during the mesh when one pair of teeth will be taking the entire load. However, these will occur toward the center of the mesh region where the load is applied at a lower position on the tooth, rather than at its tip. This point is called the highest point of single-tooth contact or HPSTC. Gears should not generally be designed having contact ratios less than about 1.2, because inaccuracies in mounting might reduce the contact ratio even more, increasing the possibility of impact between the teeth as well as an increase in the noise level. Thus, even though a contact ratio of 1.2 is acceptable, a minimum contact ratio of 1.4 is preferred, and larger is better. Most spur gear sets will have contact ratios between 1.4 and 2. [Sabah M.J. Ali, 2007, Ali Raad, 2009] For normal contact ratio gearing the number of meshing teeth alternates between one and two.

Figure (3.4b) shows a gear mesh with the driving pinion tooth on the left just coming into contact at point (A) and the two teeth on the right in contact at point S. Notice that contact starts at point (A) the highest point of contact on the gear tooth where the outside diameter of the gear crosses the line of action and ends where the outside diameter of the pinion crosses the line of action at point (B) the lowest point of contact on the gear tooth. AB in the figure is the length of contact line.

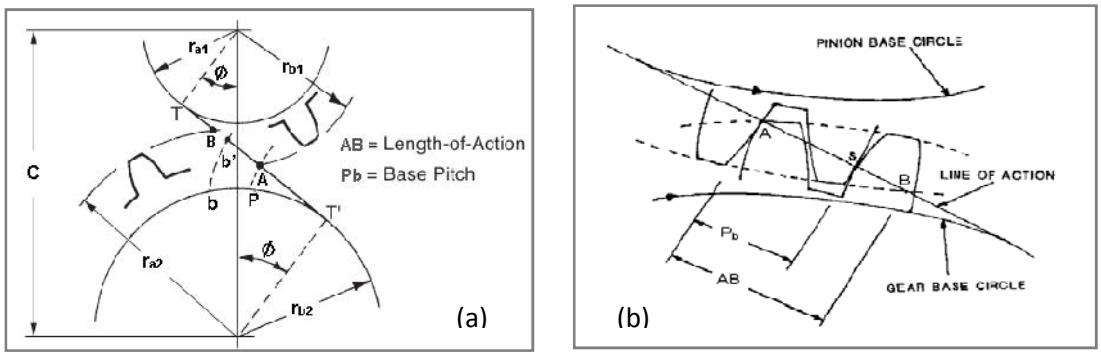

Figure 3.4: Gear teeth action

The contact ratio, *CR* is calculated from:

$$CR = \frac{\overline{AB}}{P_b} \qquad 3.41$$

Where, $\overline{AB}$ is the length of line of action, and P_b is the base pitch.

In normal contact ratio gearing, the load is transmitted by single pair of teeth for part of the period of engagement, and by two pair of teeth during rest of the period. Where as in the beginning of contact there are two pair in contact continuing in meshing for a specified period then one of them goes out of contact, and the other pair continues in meshing alone, until a new pair comes into action [Maitra G.M.,1997]. For example a contact ratio of (1.6) means that in the beginning of the path of contact, there are two pairs continuing in meshing 60% of the base circular pitch along the path of contact. Then one pair goes out of contact and the other pair continues in meshing alone for the rest 40% of the base circular pitch, after this a new other pair comes into contact. By this method the engagement will be repeated, as shown in figure (3.6b).

Contact ratios for conventional gearing are generally in the range (1.4 – 1.6). The zone of action of meshing gear teeth shown in Figure (3.5), that tooth contact begins and ends at the intersection points of the two addendum circles with the pressure line (line of action). The distance along the line of action between these points within the mesh is called the length of action AB. In Figure (3.5) initial contact occurred at A ends at B. As shown in figure, the distance aP is called the arc of approach qa, and the distance Pb is the arc of recess qr. And the sum of these is the arc of action qt.

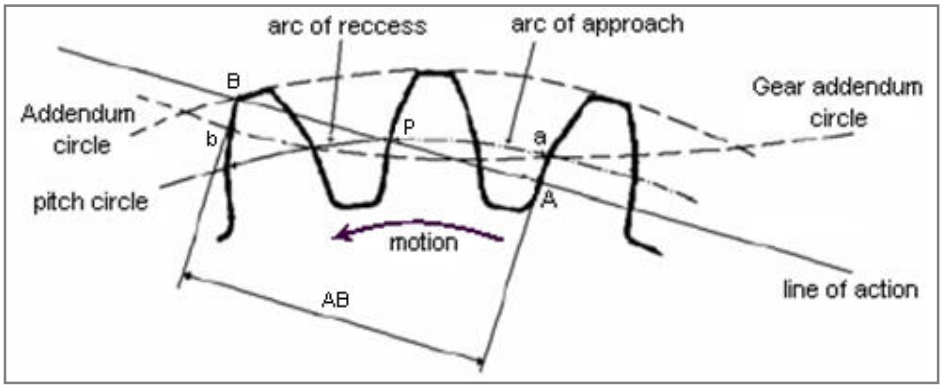

Figure 3.5: Approach and recess action

3.4.1 The Contact Ratio Analysis

Now, considering a situation in which the arc of action is exactly equal to the circular pitch Pc, that is, $qt = Pc$. This means that one tooth and its space will occupy the entire arc ab. In other words, when a tooth is just beginning contact at A, the previous tooth is simultaneously ending its contact at B. Therefore during the tooth action from A to B, there will be exactly one pair of teeth in contact. Next, considering a situation in which the arc of action is greater, let $qt = 1.6\,Pc$. This means that when one pair of teeth is just entering contact at A, another pair, already in contact, will not yet have reached B. Thus, for some period of time, there will be two teeth in contact, one in the vicinity of a and another near b. As the meshing proceeds, the pair near b must cease contact, leaving only a single pair of contacting teeth, until the procedure repeats itself. Because of the nature of this tooth action, since either one or two pairs of teeth are in contact, it is convenient to define the term contact ratio CR as:

$$CR = \frac{q_t}{p_c} \qquad 3.42$$

Where, q_t is the arc of action. Note that this ratio is also equal to the length of the path of contact divided by the base pitch. An easier way to obtain the contact ratio is to measure the line of action AB instead of the arc distance ab. Since AB in Figure (3.5) is a tangent to the base circle when extended, the base pitch P_b must be used to calculate CR instead of the circular pitch P_c [Shigley J.E., 2006], as in Equation (3.41).

Referring to Figure (3.4b), the positions of the end points of the path of contact are then as follows [Colbourne J.R. (1987)]:

$$S_A = -r_{b1}tan\phi + \sqrt{(r_{a1})^2 - (r_{b1})^2} \quad 3.43$$

$$S_B = r_{b2}tan\phi - \sqrt{(r_{a2})^2 - (r_{b2})^2} \quad 3.44$$

Where, r_{b1} and r_{b2} are the base radii of pinion and gear and r_{a1} and r_{a2} are the outer radii of pinion and gear respectively. Another useful equation to obtain the value of working pressure angle ϕ is:

$$\cos(\phi) = \frac{r_{b1} + r_{b2}}{C} \quad 3.45$$

Where, C is the center distance

So,

$$AB = S_A - S_B \quad 3.46$$

$$\overline{AB} = \sqrt{(r_{a1})^2 - (r_{b1})^2} + \sqrt{(r_{a2})^2 - (r_{b2})^2} - (r_{b1} + r_{b2})tan\phi$$

or

$$\overline{AB} = \sqrt{(r_{a1})^2 - (r_{b1})^2} + \sqrt{(r_{a2})^2 - (r_{b2})^2} - (r_{p1} + r_{p2})sin\phi$$

By substituting in equation (3.34), CR can be written as:

$$CR = \frac{1}{P_b}\left|\sqrt{(r_{a1})^2 - (r_{b1})^2} + \sqrt{(r_{a2})^2 - (r_{b2})^2} - (r_{b1} + r_{b2})tan\phi\right| \quad 3.47$$

But substituting $P_b = 2\pi R_P \cos\phi / N$, $r_a = R + a$, and $r_b = R\cos\phi$, equation (3.47) will become:

$$CR = \frac{\sqrt{(R_P + a)^2 - R_P^2 cos^2(\phi)}}{\pi m \cos(\phi)} + \frac{\sqrt{(R_G + a)^2 - R_G^2 cos^2(\phi)} - (R_P + R_G)sin(\phi)}{\pi m \cos(\phi)}$$

Where

R_P and R_G : are the operating pitch radius of the pinion and gear respectively,

ϕ: is the operating pressure angle;

m: is the module and a is the addendum (based on the operating pitch radius) which is equal to one module for standard gears.

From above equations the value of contact ratio must be greater than (1.0) provided the length of path of contact is greater than base pitch (P_b). The operation of the gears is impossible unless the value of (CR) is at least (1.0) and in general the higher value of CR makes the gear pair runs smoothly. However, for spur gears a contact ratio of at least (1.4) is generally recommended. Referring to Figure (3.5) the angle corresponding to the arc of action or to the length of path of contact can be found by calculating the angle of approach and the angle of recess. Where the angle of approach is given by [Colbourne J.R., (1987)]:

$$\phi_{App} = \frac{-S_A}{r_{b1}} \qquad 3.48$$

The angle of recess is:

$$\phi_{Rec} = \frac{S_B}{r_{b1}} \qquad 3.49$$

So, the rolls angle ϕ_c (the angle corresponding to the arc of action or to the length of path of contact) from the first point of contact A to the last point of contact B of one pair of teeth at contact operation is:

$$\phi_c = \phi_{App} + \phi_{Rec} \qquad 3.50$$

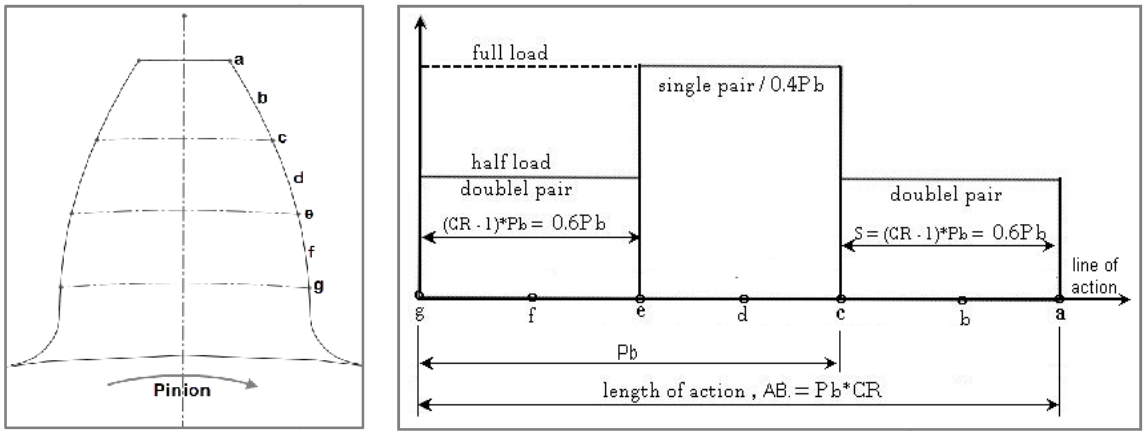

(a) (b)

Figure 3.6: Loading along the path of contact for contact ratio of 1.6

3.4.2 Design for Variable Contact Ratio Gear Pair

As it is defined above, contact ratio of a gear pair is the average number of teeth in contact during the course of engagement. [M. Rameshkumar, et al, and 2010] the contact ratio of the gear pair plays an important role in increasing the load carrying capacity of gears.

The contact ratio (CR) for any gear pair is given by equation (3.51)

$$CR = \frac{\sqrt{(R_P+a)^2-R_P^2cos^2(\phi)}}{\pi m \cos(\phi)} + \frac{\sqrt{(R_G+a)^2-R_G^2cos^2(\phi)}-(R_P+R_G)sin(\phi)}{\pi m \cos(\phi)} \quad 3.51$$

Where

R_P , and R_G : is the operating pitch radius of the pinion and gear respectively

ϕ : is the operating pressure angle;

m : is the module and a is the addendum (based on the operating pitch radius) which is equal to one module for standard gears.

High contact ratio can be achieved by different ways namely: [M. Rameshkumar, 2010]

- Increasing the number of teeth;
- Lowering the pressure angle;
- Increasing the addendum factor.

Increasing contact ratio is possible with respect to above parameters. [Durmus Gunay, 1996] Modifying the pressure angle and number of teeth can increase the contact ratio of the gear pair; but, they have disadvantage during production need for special cutting tools. In this study in order to achieve variable contact ratio for a gear pair with identical module, center distance, gear ratio and pressure angle the addendum factor of the gear pairs is increased from a standard 0.95 to 1.2. The contact ratios versus addendum factor of gear pair are calculated using a Matlab code and tabulated in figure (3.7) and table (3.1).

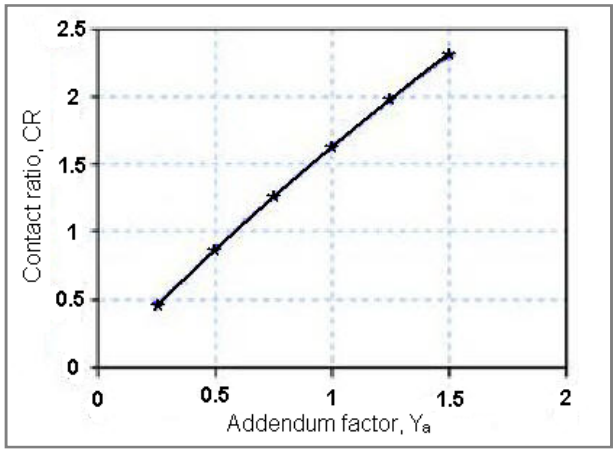

Figure 3.7: Contact ratio versus addendum factor

Table 3.1: Contact ratio

No	Addendum factor, Y_a	Addendum, $a=m*Y_a$, for m=2.5 is module	Contact ratio, CR
1	0.95	2.375	1.614
2	1.00	2.500	1.6985
3	1.05	2.625	1.7829
4	1.10	2.750	1.8673
5	1.15	2.875	1.9516
6	1.20	3.000	2.0359

3.5 Teeth Pair Load Sharing

The pinion tooth diagram shown in figure (3.6a) is marked in to 7 different alphabetical points on the right side to show how the teeth pairs come in to contact when they pass the meshing zone. This was taken from [Sabah M.J, 2007] experience. In figure (3.6b) the points are located along the line of action within the interval of length of action, AB. Considering contact ration 1.4 and above, the initial contact point for a pinion tooth with the gear tooth is point 'g', and simultaneously for the second tooth of the same pinion, which is already in mesh will be at point 'c'. In other words, the first point of action 'g' which is located on the first meshing tooth is associated with point 'c' which is located on the second meshing tooth of the same pinion. Therefore the load will be shared between these two points, similarly points 'f' and 'b', also 'e' and 'a' will have simultaneous action. Then point 'a' will goes out of contact, therefore the full load will be applied starting from point 'e', through point 'd' until the contact being at point 'c', then a new meshing tooth comes in to contact.

In normal contact ratio gearing, and when a single pair of teeth is engaged, this pair transmits the full load or the full load is then applied on the one meshing tooth only. Almost, critical conditions (for maximum generated contact stresses) occur in the one pair contact zone. When double pairs of teeth are engaged, the transmitted load will be divided between two meshing teeth. Practically the load is not divided fairly; load sharing depends on contact ratio value and stiffness of meshing tooth at point of application of load [Elkholy A.H., 1985]. In figure 3.8, the load sharing is drawn against the path of contact for normal contact ratio sharing.

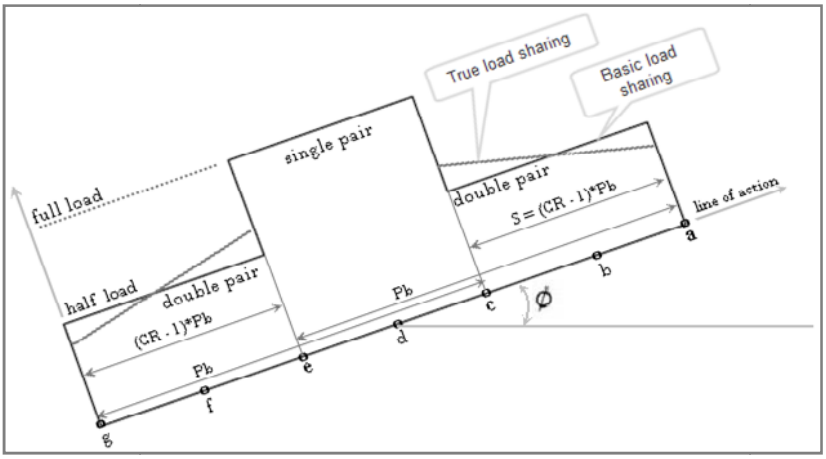

Figure 3.8: Teeth pair load sharing

3.5.1 Transmitted Load

Gears are used to transmit mechanical power and this requires applying mechanical torque that can be calculated as following

$$T = \frac{P}{\omega} \tag{3.52}$$

Then the normal load applied on meshing teeth can be found as following

$$W_n = \frac{T}{R_P \cos(\phi)} \tag{3.53}$$

The stress analysis problem in this study is assumed as a plane elastic problem, since the applied transmitted load is assumed to be distributed uniformly across the width, F of the meshing tooth. Therefore the load had been depended per unit width of tooth as following:

$$q_n = \frac{W_n}{F} \tag{3.54}$$

Thus the radial component (W_t) of the normal load W_n will be

$$W_t = W_n \cos(\phi) = q_n F cos(\phi) \tag{3.55}$$

As explained earlier, when the contact ratio changes, the path of contact and the load sharing will be changed too. To explain how to determine the location of the critical load and the angular position of the meshing tooth for each case of contact ratio, see figure (3.8). As mentioned previously, the highest stress which leads to pitting occurs at the critical loading position. Therefore meshing from point 'c' to point 'e'

causes full applied loading on the tooth face in contact that leads to a maximum generated stresses near to and at the pitch circle area. Hence, the load applied on between these points is the critical load. That means either of these points is called the highest point of single tooth contact (HPSTC) since meshing at the point creates the largest possible fatigue contact stress with single tooth contact whenever contact ratio of the paired gearing is below 2.

However, when the contact ratio is being 2 the load sharing of the paired gear teeth will be different from what is discussed above. For this reason the load sharing at point 'd', which is critical position for this case, will be less than the full load of the total transmitted load but when we go far from it the sharing may not be the same. Hence normal force W_n will be less than of its value in eq. (3.53).

3.6 Involute Spur Gear Geometry

The definition of an involute is the spiraling curve traced by the end of an imaginary taut string unwinding itself from a stationary circle called base circle. The majority of spur gears used in industrial machinery are gears with involute tooth profile. The popularity of the involute tooth profiles derived from many of its advantages, such as simplicity of design and ease of use [R.S. Khurmi, et al., 2005]. In connection with toothed wheels, the circle at which the involute curve generated is the base circle. To generate the profile is required to provide the diametral pitch, pitch diameter, pressure angle and number of divisions that are desired in the profile. This allows convenient control of the tooth geometry.

3.6.1 Involute and Evolute (Spur Gear Teeth Profile)

Consider that a planar curve I is given Figure (3.9a). Segments M_iN_i $(i = 1, 2, \ldots, n)$ represent the curvature radii of curve I at points M_i, where N_i is the curvature center. The locus of curvature centers N_i is the evolute E to curve I. The main features of E, evolute to curve I, are as follows:

- The normal M_iN_i at point M_i of curve I is the tangent to the evolute E.
- The evolute to a regular curve I is the envelope to the family of normals M_iN_i to I.

Considering E as given, we may determine the involute I for E as the result of development of E. Let us imagine an inextensible thread MN that is wrapped on curve E. Point M of the thread will trace out the involute I while the thread is wound on and off.

Consider the particular case when the evolute E is a circle. The involute I for such a case is the tooth profile for a spur gear. The evolute, the circle of radius r_b Figure (3.9b) is called the base circle. Two branches of an involute curve are shown in Figure (3.9b). They are generated by point M_o of the straight line that rolls over the base circle clockwise and counterclockwise, respectively. Each branch represents its respective side of the tooth figure (3.10).

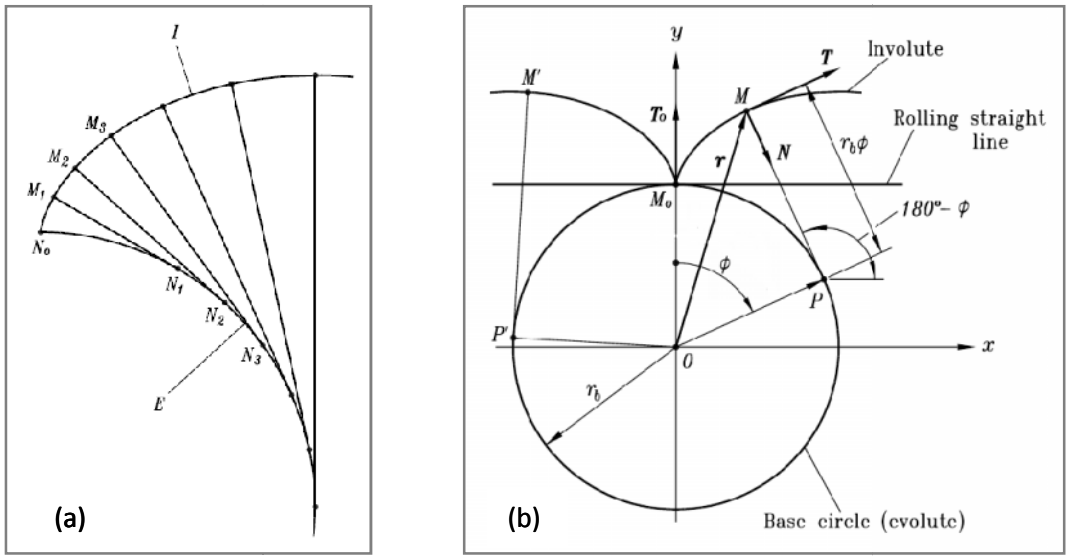

Figure 3.9: Geometry of Involute curves: (a) involute and evolute, (b) for derivation of the equation of involute curves

The analytical representation of an involute curve is based on the following considerations Figure (3.9b).

(i) A current point M of the involute curve is determined by the vector equation

$$\overline{OM} = \overline{OP} + \overline{PM} \qquad 3.56$$

Where

$$\overline{OP} = r_b[sin\phi \quad cos\phi]^T \qquad 3.57a$$

$$\overline{PM} = PM[-cos\phi \quad sin\phi]^T \qquad 3.57b$$

(ii) Due to rolling without sliding, we have

$$PM = \widehat{M_oP} = r_b\phi \qquad 3.58$$

Here, ϕ is the angle of rotation in rolling motion.

(iii) Equations (3.56) to (3.59) yield

$$x = r_b(sin\phi - \phi cos\phi) \qquad 3.59a$$

$$y = r_b(cos\phi + \phi sin\phi) \qquad 3.59b$$

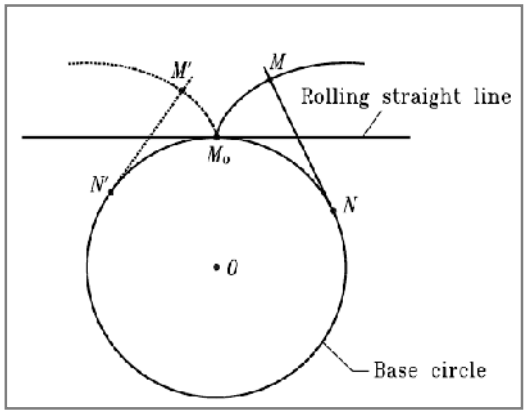

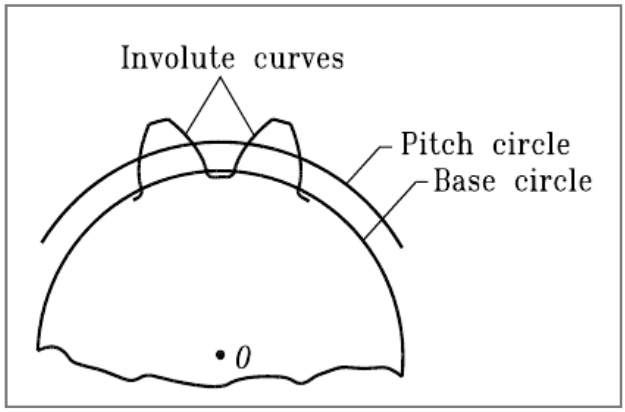

Figure 3.10: Two branches of an involute curves

3.6.2 Theoretical (AGMA) Results

Six different contact ratio gearing has obtained in section (3.4.2) for the model shown in figure (4.2). According the AGMA gear formulas, equation (3.37) to (3.40) the results of critical point (discussed in chapter 5) of the six different contact ratio gearing are tabulated in the tables below for the spur gear with parameters described in table (4.1). In table (3.2) pitting resistance and in table (3.3) stress cycle factor number of load cycles and safety factor for pitting results are tabulated.

Table 3.2: Pitting resistance

Contact Ratio	Critical loading operating diameter of pinion [mm]	Transmitted tangential load, W_t [N]	Pitting resistance (Contact Stress) [MPa]
2.0	57.50	588.7N	5.57037E+08
1.9516	57.50	817.39N	6.56374E+08
1.8673	57.33	872.14N	6.79005E+08
1.7829	57.12	875.35N	6.81503E+08
1.6985	56.92	878.43N	6.83899E+08
1.614	56.73	881.37	6.86189E+08

Table 3.3: Stress cycle factor and Safety factor for pitting

Contact Ratio	Stress cycle factor for pitting resistance	No of load cycles expected by pitting	Hours of expected fatigue life time	Safety factor for pitting
2.00	0.813475441	3.98904E+08	110806.6491	37.94748257
1.9516	0.958544078	2.12928E+07	5914.654131	2.025566483
1.8673	0.991593069	1.16238E+07	3228.845883	1.105769138
1.7829	0.99524068	1.08861E+07	3023.929482	1.035592288
1.6985	0.998740094	1.02248E+07	2840.212604	0.972675549
1.614	1.002083914	9.63234E+06	2675.650045	0.916318509

CHAPTER FOUR

4 FINITE ELEMENT ANALYSES

A new method, Finite Element Analysis (FEA) is used extensively nowadays for calculations of the strength and deflections of mechanical engineering components including gear teeth. Once these techniques were only used by big companies due to their complexity and price, but with the development of computer technology they have become more and more accessible to small gear companies, which are the majority of participants in the market [Vanyo Kirov, 2011].

[Faydor L. et al., 2004] discussed that the finite element analysis allows us to perform; stress analysis, investigation of formation of gear contact, detection of severe areas of contact stresses inside the cycle of meshing. The contact conditions are sensitive to the geometry of the contacting surfaces, which means that the finite element mesh near the contact zone needs to be highly refined. Finer meshing generally leads to a more accurate solution, but requires more time and system resources [P. Kumar, 2009]. It is recommended not to have a fine mesh everywhere in the model to reduce the computational requirements.

To perform this application, developing of finite element mesh of the gear drive, defining the contact surfaces of the teeth pair and establishing the boundary conditions of the loading of the gear drive are carried out before the analysis is performed in ANSYS 14. This procedure is deployed to generate the finite element model as seen in figure (4.1) after the 3D model generated in CATIA V5R16 and assembled in Solid Works 10 is imported to ANSYS 14.0.

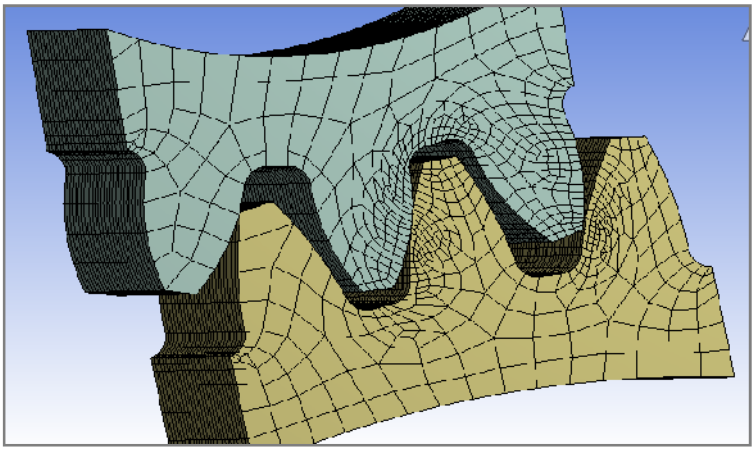

Figure 4.1: Meshed spur gear teeth pair

A free and mapped meshing capability of ANSYS Workbench is employed to generate the finite element mesh. Refinement in the contact region is performed using contact sizing option. Then, the meshing performed to generate the finite elements. The finite element mesh is generated in such a way that to decrease element size at the contact region (maximum stress region), increase the size of the elements when moving away from the contact region, so that there will be, More number of small size elements in the contact region and less number of elements in low stress regions respectively to reduce the computation time and computer memory requirement, within reasonable accuracy.

4.1 Generation of Spur Gear

The spur gear pair with the properties given in table (4.1) is chosen to model the problem at hand. Using these parameters and the involute curve equations (3.59a, and 3.59b), the solid models created in CATIA V5R16. In order to generate involute profile in CATIA, five key points are created in the range of Dedendum and Addendum circle radii representing the involute profile using equation (3.59a, and 3.59b). These points represent radii values in the range of Dedendum and Addendum circle. All these radii values are connected with spline, in generative shape design modeler. Once the involute shape is generated, by using extrapolation, reflection, and array command the 3D model is developed. Then the 3D model is imported to Solid Works 10 for assembling, and after that it is imported to ANSYS workbench for the purpose of finite element analysis. However, to minimize computation time, only a three pairs of meshed teeth model is imported to ANSYS Workbench 14.0 to carry out the analysis.

Table 4.1: Spur Gear Parameters

Parameters	**pinion**	**gear**
Module, m [mm]	2.5	2.5
Pressure angle, ϕ [deg]	20	20
Number of teeth, z	23	45
Face width, b [mm]	10	10
Pitch circle diameter, D [mm]	57.5	112.5
Materiality	Chromium-molybdenum alloy steel (SCM 420)	Chromium-molybdenum alloy steel (SCM 420)
Modules of elastic [GPa]	206	206
Poisson's ratio	0.3	0.3
Applied torque [Nm]	25	
Center distance [mm]	85	

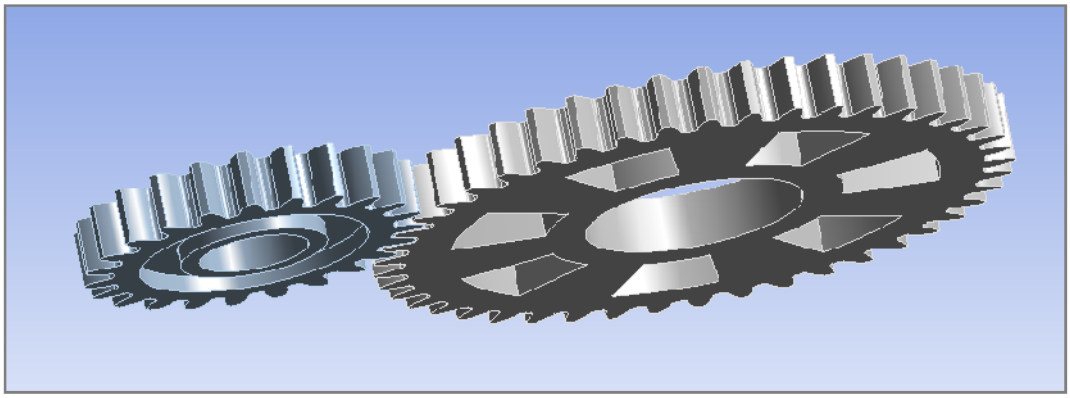

Figure 4.2: Meshed Spur Gear

4.2 ANSYS Contact Models

ANSYS supports five contact models: node-to-node, node-to-surface, surface-to-surface, line-to-line, and line-to-surface. But in general, there are three basic types of contact modeling application as far as ANSYS use is concerned [ANSYS V14.0, 2011]. Each type of model uses a different set of ANSYS contact elements and is appropriate for specific types of problems.

1) Point-to-point contact: the exact location of contact should be known beforehand. These types of contact problems usually only allow small amounts of relative sliding deformation between contact surfaces.
2) Point-to-surface contact: the exact location of the contacting area may not be known beforehand. These types of contact problems allow large amounts of deformation and relative sliding. Also, opposing meshes do not have to have the same discretisation or a compatible mesh.
3) Surface-to-surface contact is typically used to model surface-to-surface contact applications. The finite element model recognizes possible contact pairs by the presence of specific contact elements. These contact elements are overlaid on the parts of the model that are being analyzed for interaction. In this study two faces of the contacted teeth pairs are taken to employee the surface-to-surface contact.

4.2.1 Surface-to-Surface Contact Elements

There are many types of contact problems that may be encountered, including contact stress, dynamic impacts, metal forming, bolted joints, crash dynamics, assemblies of components with interference fits,

etc. All of these contact problems, as well as other types of contact analysis, can be split into two general classes (ANSYS),

1. Rigid - to - flexible bodies in contact,
2. Flexible - to - flexible bodies in contact

In rigid - to - flexible contact problems, one or more of the contacting surfaces are treated as being rigid material, which has a much higher stiffness relative to the deformable body it contacts. Many metal forming problems fall into this category. Flexible-to-flexible is where both contacting bodies are deformable. Examples of a flexible-to-flexible analysis include gears in mesh, bolted joints, and interference fits.

ANSYS supports both rigid-to-flexible and flexible-to-flexible surface-to-surface contact elements. These contact elements use a "target surface" and a "contact surface" to form a contact pair.

In problems involving contact between two boundaries, one of the boundaries is conventionally established as the "target" surface, and the other as the "contact" surface. For rigid-flexible contact, the target surface is always the rigid surface, and the contact surface is the deformable surface. For flexible-to-flexible contact, both contact and target surfaces are associated with the deformable bodies. These two surfaces together comprise the "contact pair." For 3-D contact pairs, TARGE170 with CONTA174 are used for the surfaces in contact. Each contact pair is identified via the same real constant number. To create a contact pair, the same real constant number to both the target and contact elements is assigned as per the software command permits.

Contact elements are constrained against penetrating the target surface. However, target elements can penetrate through the contact surface. For rigid-to-flexible contact, the designation is obvious: the target surface is always the rigid surface and the contact surface is always the deformable surface. For flexible-to-flexible contact, the choice of which surface is designated contact or target can cause a different amount of penetration and thus affect the solution accuracy. To maintain the accuracy of solution the following guidelines are considered when designating the surfaces:

- If a convex surface is expected to come into contact with a flat or concave surface, the flat/concave surface should be the target surface.
- If one surface has a fine surface mesh and, in comparison, the other has a coarse mesh, the fine mesh should be the contact surface and the coarse mesh should be the target surface.
- If one surface is stiffer than the other, the softer surface should be the contact surface and the stiffer surface should be the target surface.
- If higher-order elements underlie one of the external surfaces and lower-order elements underlie the other surface, the surface with the underlying higher-order elements should be the contact surface and the other surface should be the target. However, for 3-D node-to-surface contact, the lower-order elements should be the contact surface. The higher-order elements should be the target surface.
- If one surface is markedly larger than the other surface, such as in the instance where one surface surrounds the other surface, the larger surface should be the target surface.

4.2.2 ANSYS Contact Algorism

Various algorithmic procedures have been proposed to solve contact problems in finite element analysis. Most of these procedures are based on penalty and Lagrange multiplier techniques, for enforcing the contact constraints. ANSYS uses four different contact algorithms: pure penalty method, Augmented Lagrangian method, Pure Lagrangian multiplier method and Lagrangian multiplier on contact normal and penalty on frictional direction and for the study in hand the Augmented Lagrangian method is applied.

The augmented Lagrangian method is an iterative series of penalty updates to find the Lagrange multipliers (i.e., contact tractions). Compared to the penalty method, the augmented Lagrangian method usually leads to better conditioning and is less sensitive to the magnitude of the contact stiffness coefficient. However, in some analyses, the augmented Lagrangian method may require additional iterations, especially if the deformed mesh becomes excessively distorted. The contact pressure is defined by:

$$P = \begin{cases} 0 & if \quad U_n > 0 \\ K_n U_n + \lambda_{i+1} & if \quad U_n \leq 0 \end{cases}$$

Where $\lambda_{i+1} = \begin{cases} \lambda_i + K_n U_n & if\ |U_n| > \varepsilon \\ K_n U_n + \lambda_{i+1} & if\ |U_n| \leq \varepsilon \end{cases}$

ε= compatibility tolerance (input as FTOLN)

- FTOLN is a factor based on the thickness of the element which is used to calculate allowable penetration.

λ_i = Lagrange multiplier component at iteration i

The Lagrange multiplier component λ_i is computed locally (for each element) and iteratively.

4.2.3 The Employed ANSYS Analysis Steps

To come up the final result different steps are used, starting from modeling the spur gear in CATIA to stress analysis of the model in ANSYS workbench. Although the steps used are many, to make general summary they are classified into five as discussed below. [Solomon, 2011] has utilized similar steps in his study.

a. The model is generated using the equations of involute profile for spur gear tooth, (for both the pinion and the gear), in CATIA V5R16. Then, after assembling the model in Solid Works 10, three pairs of gear teeth is imported in to ANSYS Workbench 14.0 as working model. As discussed earlier the involute curve is generated using equations (3.59a and 3.59b), so as the loss of accuracy associated with development of solid models using computer aided design programs is minimized.

b. Modules for automatic generation of finite element models are integrated into the model in ANSYS Workbench version 14.0, static structural analysis system. Then, the generation of finite element models is accomplished for the cycle of meshing.

c. Define material properties which are necessary to solve the problem. Here the gear material is 16MnCr5 and the required material properties for this analysis are only Modulus of elasticity, Poison's Ratio and Density. The Modulus of elasticity of 16MnCr5 is 206 GPa. The Poison's Ratio of 16MnCr5 is 0.3. The Density of 16MnCr5 is 7850 kg/m3.

d. To get the contact stresses the contact wizard is used in ANSYS Workbench. The contact algorithm in ANSYS Workbench computer program requires definition of contacting surface. To define a contact pair completely, contact and target element are referred to same characteristic parameters as

CONTA174 and target170. Then, augmented Lagrangian method contact algorithm, with frictionless contact is used.

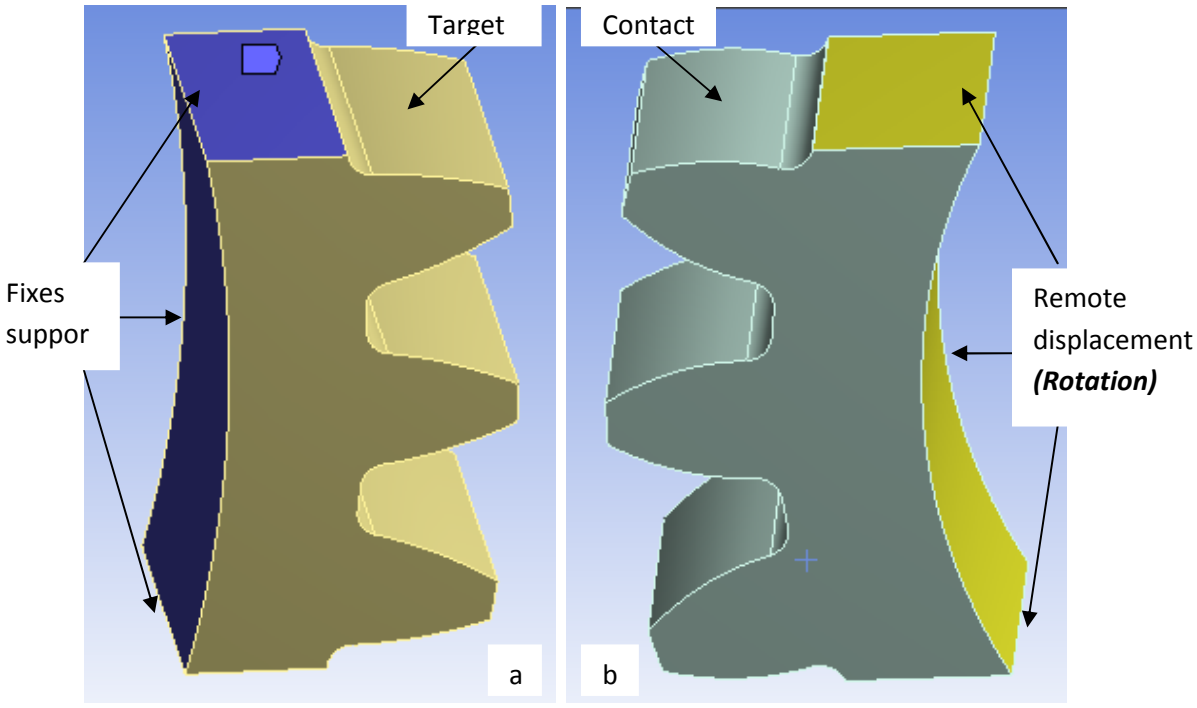

Figure 4.3: The Boundary Conditions of the Paired Spur Gear Teeth: (a) Gear, (b) Pinion

e. The boundary conditions for gear and pinion is performed as follows: Nodes on the sides and bottom part of the rim portion of the gear are considered as fixed support Figure (4.2a). Nodes on the two sides and bottom part of the rim portion of the pinion built as rigid remote displacement Figure (4.2b).

Rigid surfaces are three-dimensional geometric structures that cannot be deformed but can perform translation or rotation as rigid bodies. The rigid body reference node is located on the pinion axis of rotation with all degrees of freedom fixed to zero, except the rotation around the axis of rotation of the pinion. The torque is applied directly to the remaining degree of freedom of the rigid body reference node, see figure (5.1a).

CHAPTER FIVE

5 RESULT AND DISCUSSION

5.1 Estimation of Percentage Load Sharing

Each Gear is meshed at center distance of 85 mm, where the pitch diameter of pinion and gear become tangent to each other. Six models which have different contact ratio are taken for analysis. Each gear is rotated as a rigid body according to the gear ratio to obtain the different properties of the meshed spur gear teeth pair during the power transmission. The solution is repeated for each contact ratios of the spur gears rotated with same amount of angular increment according to the gear ratios. The six models are with the same gear ratio for they are with the same pitch diameter, number of teeth but different contact ratio due to different addendum factor (contact ratio is directly proportional with addendum factor).

Approximately 15 angular increments with 1.5 degree steps are used for this analysis and the analysis is carried out with the help of the ANSYS Workbench. Load sharing ratio, the contact stress and other properties are obtained for all the gear mesh positions. The nodal forces at each node of the contact element are obtained from the ANSYS workbench post processing for each individual meshed gear tooth of the pinion during application of load. By this methodology, the percentages of load sharing between a pair of teeth are estimated for all the gear pairs throughout the path of contact.

Accordingly, the maximum percentages of load shared by the individual teeth for the normal contact ratio gears are estimated for the entire path of contact. The individual tooth loads have been determined by comparing the total normal load to the sum of the normal loads contributed by each pair of contact equally. For each contact ratios the load sharing percentage of the pinion spur gear tooth versus to radial rotation angle is shown on the figures (5.2) to (5.7).

5.2 Load Sharing Comparison

It is observed from the section (3.7.1) that for the Normal Contact Ratio, CR < 2 gearing the maximum load of 100% is taken by the single tooth at the HPSTC point (Highest point of single tooth contact) and at the tip of teeth only 40.2% load is shared for the contact ratio of 1.614 gear pair. In this case there is double teeth and single tooth engagement interchange during the course of power transition. Therefore the maximum load is applied during the single tooth contact which leads for maximum pitting nearby and at the pitch circle. However, for the High Contact Ratio (contact ratio of 2) gearing the maximum load of 67.7% load is taken at the FLPDTC (First lowest point of double tooth contact) which is right at the pitch circle and only 33.7% load is shared at the tip of the teeth during the course of engagement. In the study in hand for the contact ratio below two the maximum load (100% of full load) is applied near and at the pitch circle, and for the contact ratio of two the maximum load applied is about 67.7% of the full load.

Load sharing ratios in terms of percentage load shared from root to tip of a particular tooth of normal contact ratio gearing 23/45 are shown in the Figures listed from figure (5.2) to (5.7). The load sharing ratio is plotted with respect to rotation angle for a single tooth of the 23 gear tooth from root to tip which corresponds to a radial rotation angle of the pinion gear.

In the contact ratio of 1.614 gearing as shown in figure (5.2) for percentage load sharing the corresponding rotation angle is between 2.25 deg (tip) and 20.43 deg (root).

As it is shown in figure (5.2) the double tooth contact range is from 2.25 deg to 9.05 deg and from 14.25 deg to 20.43 deg while the single tooth contact band starts from 9.05 deg and ends at 14.25 deg. The maximum and minimum percentage of load shared in the double tooth contact bands are 59.98% and 40.2% respectively, which is gradual rate of increase. In the entire range of the single tooth contact, 100% load is carried by the single tooth despite the load between the rotations 9.05 deg and 9.75 deg suddenly increases from 59.98 to 100% during the change over from double tooth to single tooth. Similarly

between the rotations 13.55 deg and 14.25 deg the sharing suddenly decreases from 100% to 60% of the full load in view of single to two teeth contact and the load sharing ratio decreases gradually towards root. This phenomenon is common to any tooth of the 23 teeth gear which is in contact.

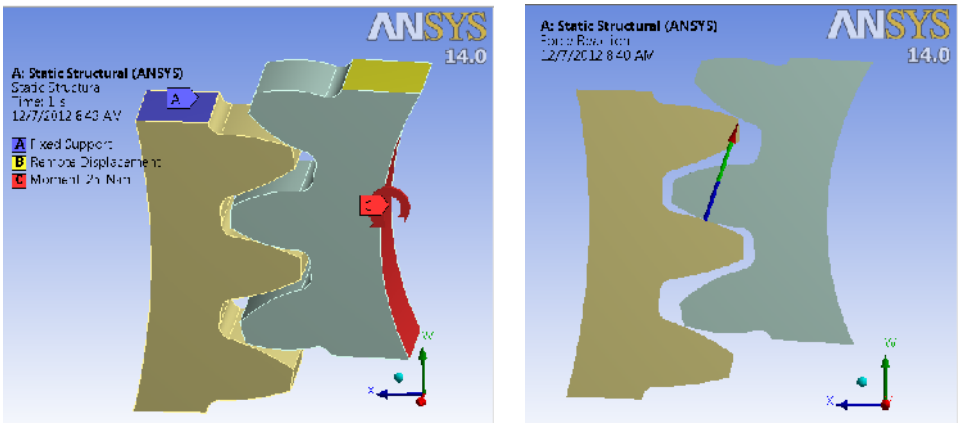

(a) (b)

Figure 5.1: Applied Torque and Reaction force: (a) Torque applied on pinion, (b) Reaction force applied on pinion tooth from gear tooth

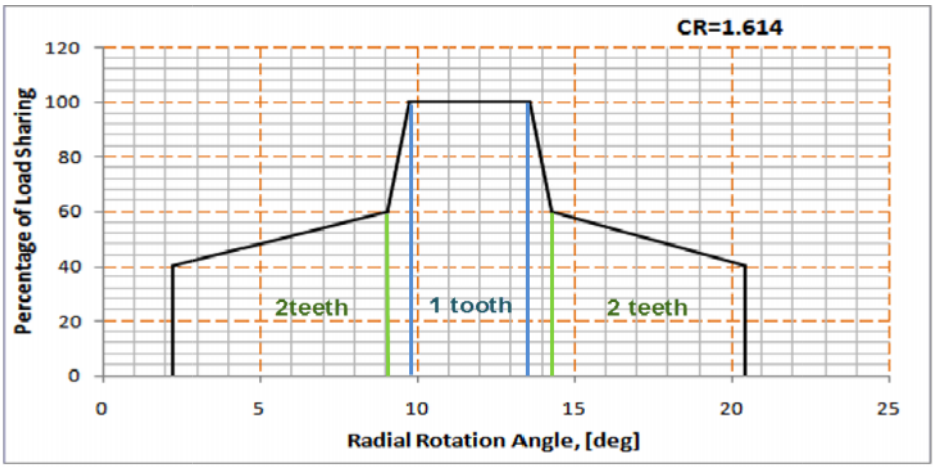

Figure 5.2: load sharing of 23/45 Teeth of Contact Ratio 1.614

In the case of 1.6985 contact ratio gearing the corresponding rotation angle for load sharing is between 1.76 deg (tip) and 20.92 deg (root).

As it is shown figure (5.3) the double tooth contact range is from 1.76 deg to 9.55 deg and from 13.76 deg to 20.92 deg while the single tooth contact range starts from 9.55 deg and ends at 13.76 deg. The maximum and minimum percentage of load shared in the double

tooth contact bands are 61.35% and 38.77% respectively. In the entire range of the single tooth contact, 100% load is taken by the single tooth except at the margins, 9.55 deg and 13.76 deg in which the load suddenly increase and decrease respectively.

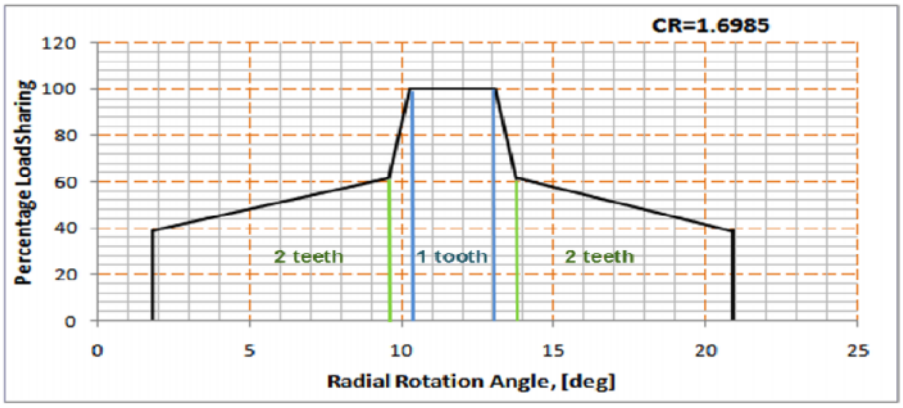

Figure 5.3: load sharing of 23/45 Teeth of Contact Ratio 1.6985

In the case of 1.7829 contact ratio gearing the corresponding rotation angle for load sharing is between 1.27 deg (tip) and 21.42 deg (root).

As it is shown figure (5.4) the double tooth contact group is from 1.27 deg to 10.04 deg and from 13.27 deg to 21.42 deg while the single tooth contact range starts from 10.04 deg and ends at 13.27 deg. The maximum and minimum percentage of load shared in the double tooth contact bands are 62.88% and 37.33% respectively. In the entire range of the single tooth contact, 100% load is taken by the single tooth.

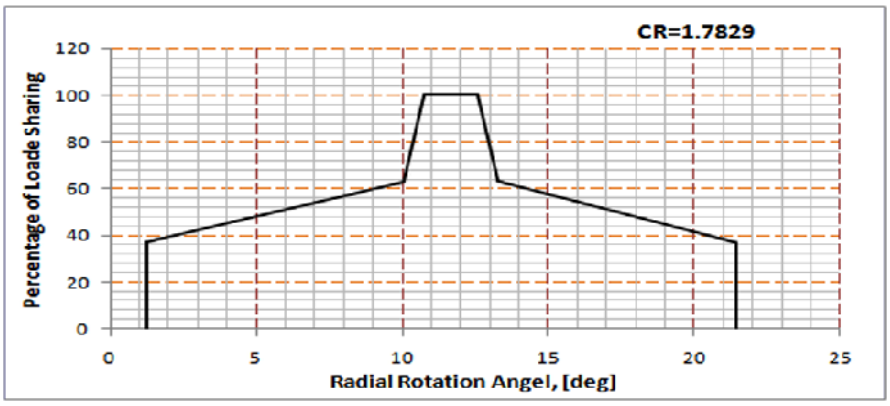

Figure 5.4: load sharing of 23/45 Teeth of Contact Ratio 1.7829

When the 1.8673 contact ratio gearing is considered the corresponding rotation angle for load sharing becomes between 0.77 deg (tip) and 21.91 deg (root).

For this case as shown figure (5.5) the double tooth contact group is from 0.77 deg to 10.53 deg and from 12.78 deg to 21.91 deg while the single tooth contact range starts from 10.53 deg and ends at 12.78 deg. The maximum and minimum percentage of load shared in the double tooth contact bands are 64.32% and 35.89% respectively. Where as in the entire range of the single tooth contact, 100% load is taken by the single tooth.

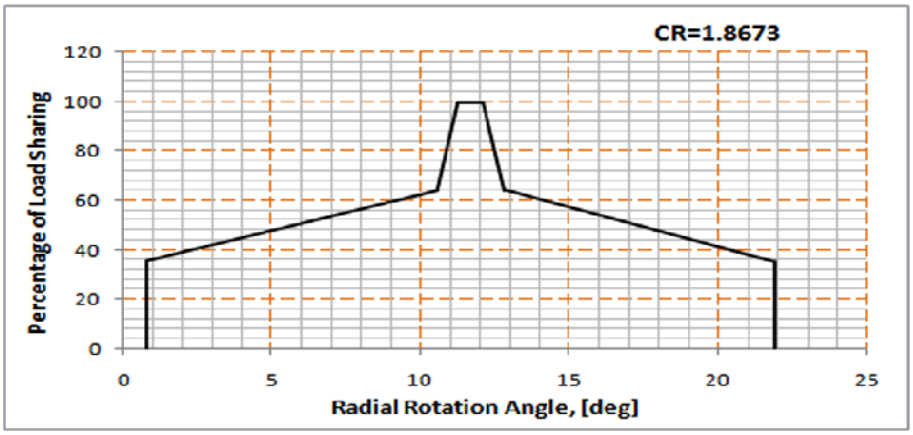

Figure 5.5: load sharing of 23/45 Teeth of Contact Ratio 1.8673

When the 1.9561 contact ratio gearing is considered the corresponding rotation angle for load sharing becomes between 0.28 deg (tip) and 22.40 deg (root).

For this case as shown figure (5.6), the double tooth contact group is from 0.28 deg to 11.02 deg and from 12.29 deg to 22.40 deg while the single tooth contact range starts from 11.02 deg and ends at 12.29 deg. The maximum and minimum percentage of load shared in the double tooth contact bands are 65.75% and 34.46% respectively. Where as in the entire range of the single tooth contact, in the range between the rotation 11.02 deg to 11.65 deg shows sudden increase from 65.75% to 94%, similarly between 11.65 deg to 12.29 deg shows sudden decrease from 94% to 65.75% of the full load.

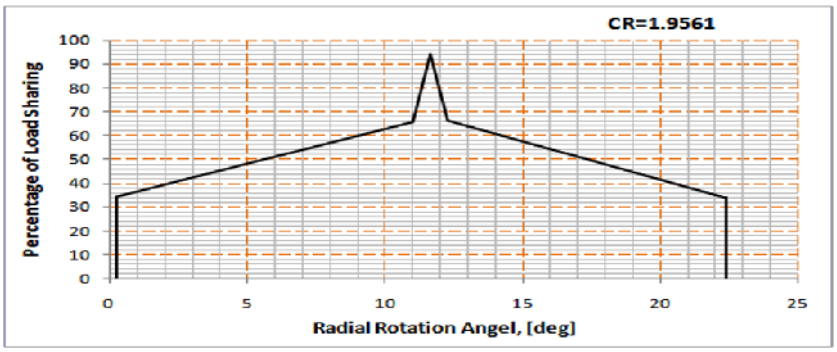

Figure 5.6: load sharing of 23/45 Teeth of Contact Ratio 1.9561

When the 2.00 contact ratio gearing is considered the corresponding rotation angle for load sharing becomes between 0.0 deg (tip) and 22.68 deg (root).

It can be seen from the graph (fig. 5.7) that the double tooth contact band is throughout the entire engagement, which is from 0.00 deg to 22.68 deg. The maximum and minimum percentage loads shared in the entire double tooth contact range are 67.66% and 33.74% respectively.

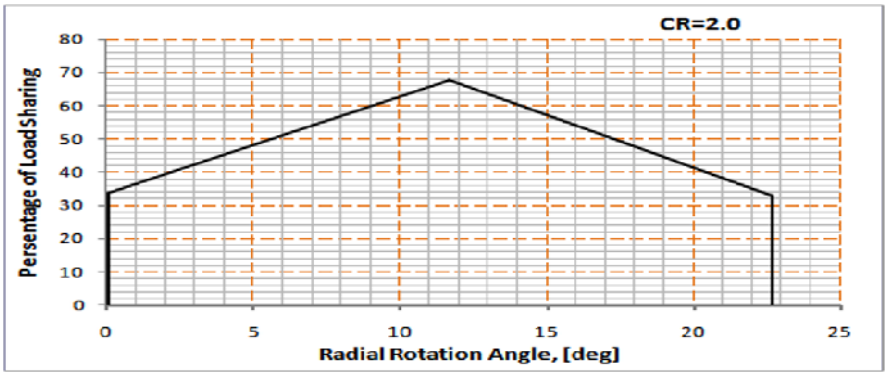

Figure 5.7: load sharing of 23/45 Teeth of Contact Ratio 2.00

5.3 Comparison of Vonmises Stress

As described in section (5.1) the maximum load which causes the higher stress on the tooth in mesh of the different gearing is on the regions, at which the single tooth carries 100% of the full load during power transmission. In this study, the Vonmises stress at the meshes was calculated based on the tooth load distributed on a unit contact area of the tooth surface. A reduction in the load sharing happens due to the increase of the addendum factor and the number of double teeth contact region, resulting in a lesser Von

Mises stress. The variation of VonMises stress on the 23 tooth normal contact ratio gear as shown in figures (5.9) resemble the load sharing behavior.

For instance if we take the 1.614 contact ratio gearing figure (5.9a), the stress varies from 227.59 MPa at the tip to 288.94 MPa at the start of single tooth contact, corresponding to 9.05 degrees, then after sudden increase to 374.75 MPa at the 9.75 degree rotation, the stress maintains to increase to 382.79 MPa till the rotation comes to 13.55 degree, then the stress goes to sudden decrease at the end of single pair teeth contact to 297.23 MPa at 14.25 degrees rotation and gradually decreases to 246.72 MPa at the root part of the teeth, in a manner similar to the load sharing pattern.

When the contact ratio comes to 2.00 gearing figure (5.9f) the maximum stress on the teeth is 311.80 MPa corresponding to 11.65 deg which is at the pitch circle. At the tip and root part of teeth the stress goes decreasing to 207.58 MPa and 229.79 MPa respectively.

In general, the load carrying capacity of the teeth increases with increasing the contact ratio of the gear. As a result the Von-mises stress is lower for the higher contact ratio gearing. However When the contact ratio is changed from (1.9) to (2.0), the decrease of stresses was more than the decrease of stresses when the contact ratio is changed between any two other successive cases.

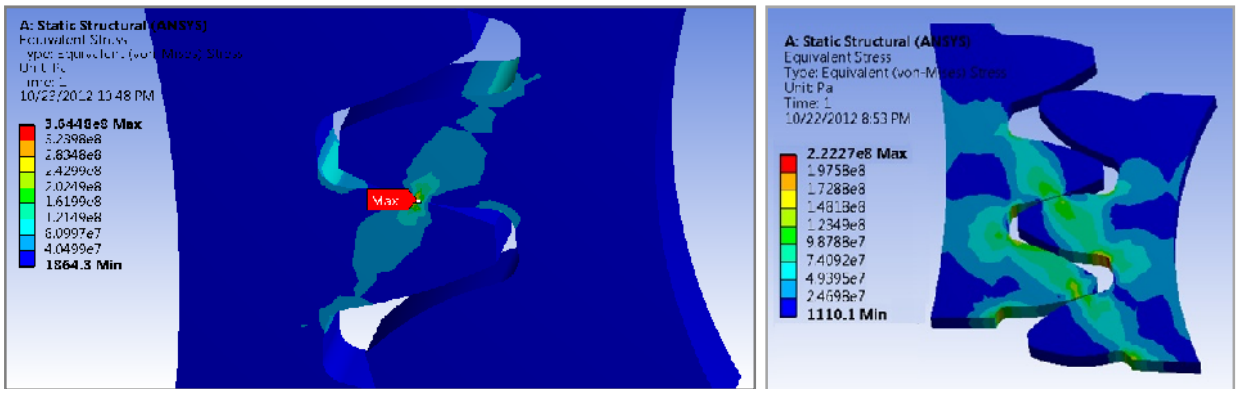

(a) (b)

Figure 5.8: Von Mises stress distribution: (a) Single pair teeth contact, (b) Double pair teeth contact

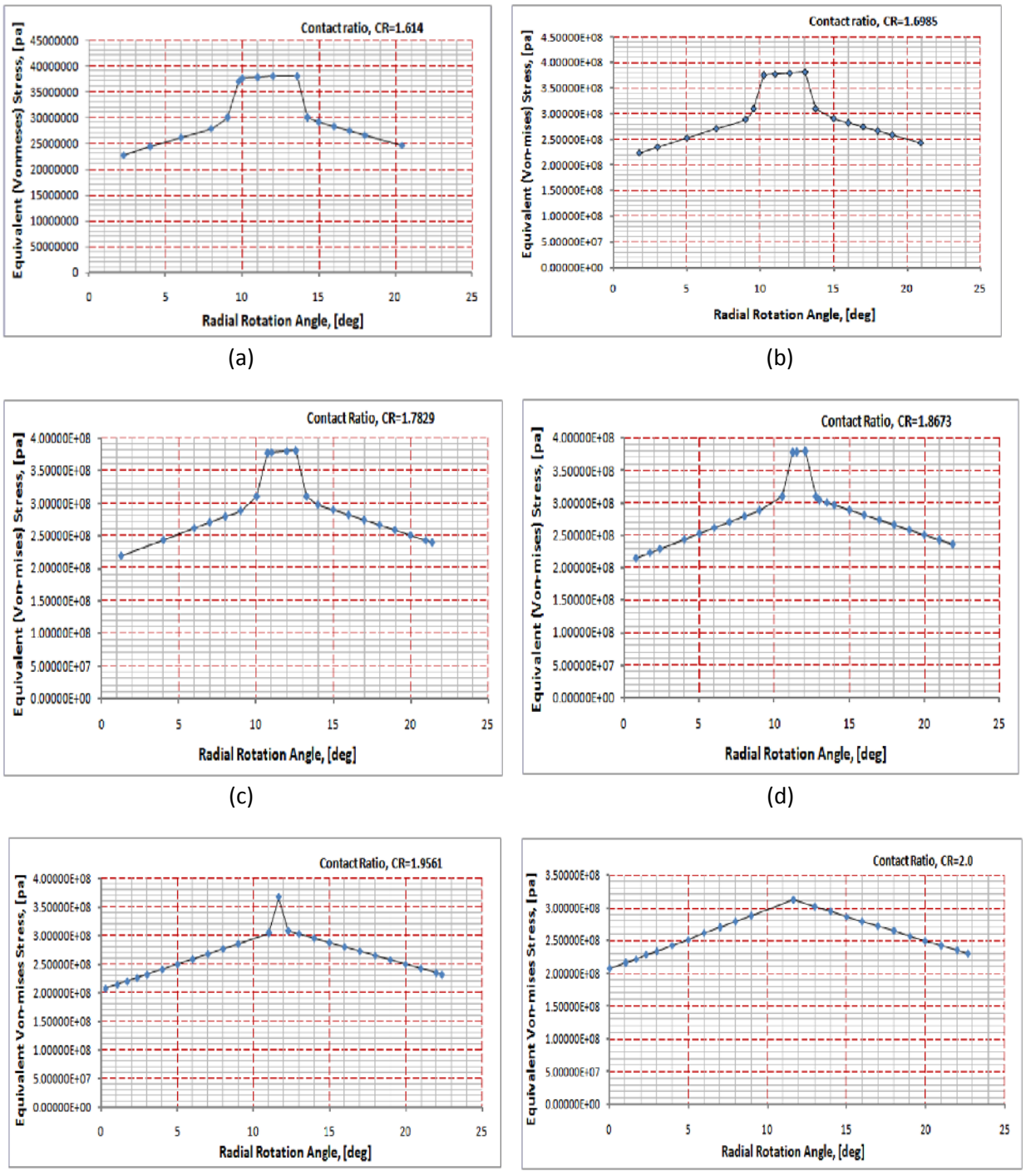

Figure 5.9: Von Mises stress of 23/45 teeth of different contact ratio gearing: (a) CR=1.614, (b) CR=1.6985, (c) CR=1.7829, (d) CR=1.8673, (e) CR=1.9561, (f) CR=2.00

5.4 Critical Point Contact Stress

When the contact ratio changes, the path of contact and the load sharing will be changed too. As explained earlier the load sharing which leads to critical loading is with in the higher load sharing region. To explain how to determine the location of the critical stress and the angular position of the meshing tooth for each case of contact ratio, see figure (3.6).

For comparison the contact stress variasion at the two ranges at which single tooth loading begines and ends (line “c” and “e” respectively) for the different contact ratio gearing is shown in figure (5.11). The contact stress at line “c” for the least contact ratio gearing (CR= 1.614) is 666.904 MPa and at line “e” is 686.189 MPa, in addition if we observe for the rest contact ratio gearing the maximum stress is at line “e”, untill the CR becomes greater and equal to 1.9561. It is clear that the meshing at line “e” with full applied load on meshing tooth, leads to a maximum generated stresses in contact area, hence the load applied on point “e” is the critical load. Meshing at point “e” creates the largest possible contact stress with single pair of teeth contact; so that point “e” is called the highest point of single tooth contact.

The space between the two points (“c” and “e”) becomes smaller as the contact ratio of the gears goes larger untill contact ratio of 1.95, figure (3.6). Beyond contact ratio 1.95 gearing the two points are merged with point “d” (pitch circle). This means single pair of teeth mesh is eliminated and every contact will be between two pairs of teeth as result the load will be shared between them.

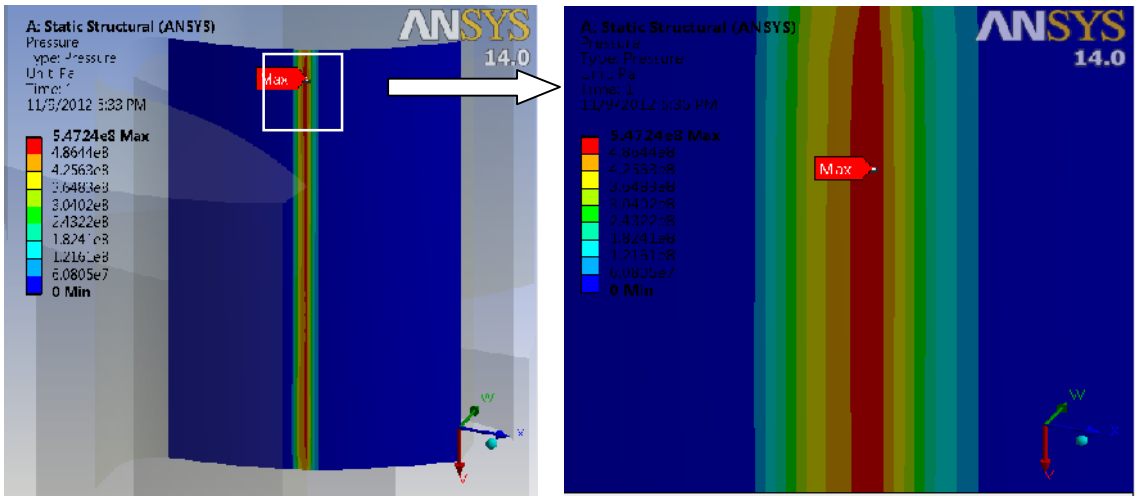

Figure 5.10: Contact Pressure distribution

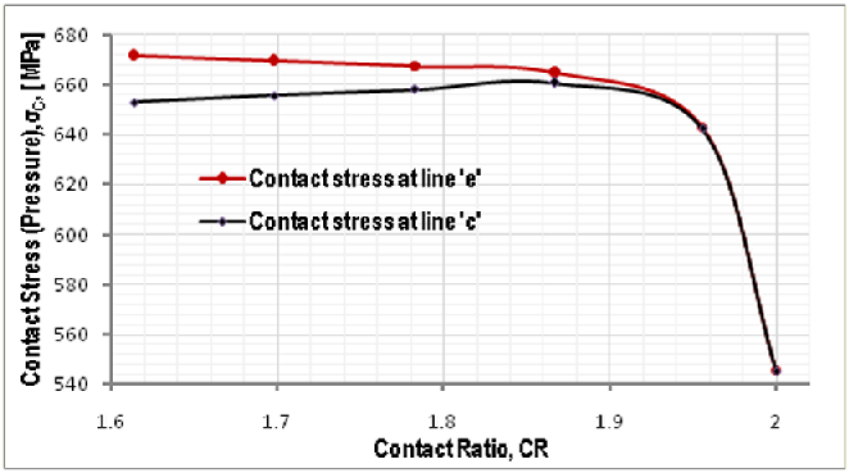

Figure 5.11: Contact stress versus Contact Ratio at line "e" and "c"

To determine location of line "e" on the path of contact, (S) must be calculated, so that the angular position of meshing tooth can be measured by angle, as shown in table (5.1).

Table 5.1: Rotation angle

Case no	Contact ratio	S of line e from line g	rotation angle from
		S= (CR-1)*Pb [mm]	tooth tip [deg]
1	1.614	4.53	13.55
2	1.6985	5.16	13.06
3	1.7829	5.78	12.57
4	1.8673	6.40	12.08
5	1.9561	7.06	11.65
6	2.0	7.38	11.65

5.5 Comparison of Theoretical (AGMA) and ANSYS (FEA) results

The theoretical (AGMA) and ANSYS Contact stress (pitting resistance) results difference for the different contact ratio gearing is shown in figure (5.12). Eventhough FEA is superior to AGMA and can be used extensively to solve different mechanical problem, it is necessary to remember that FEA has its inherent errors, and the AGMA calculations are based on empirical and proven by field experiments [Vanyo Kirov, 2011]. The results calculated from AGMA (equation) and solved in ANSYS Workbench at the critical line of contact of the pinion tooth (line "e") show a difference between 1.57% and 2.38% in contact stress, the AGMA result is higher than the ANSYS one.

Table 5.2: Contact stress between AGMA and ANSYS

Contact Ratio, CR	Contact operating diameter of pinion, [mm]	ANSYS Workbench (FEA) result 0f contact stress, [MPa]	Analytical (AGMA) result of contact stress, [MPa]	Error in percent, [%]
2.0	57.50	545.342	557.037	1.57
1.9516	57.50	642.594	656.374	1.95
1.8673	57.33	664.749	679.005	2.1
1.7829	57.12	667.195	681.503	2.19
1.6985	56.92	669.541	683.899	2.27
1.614	56.73	671.782	686.189	2.38

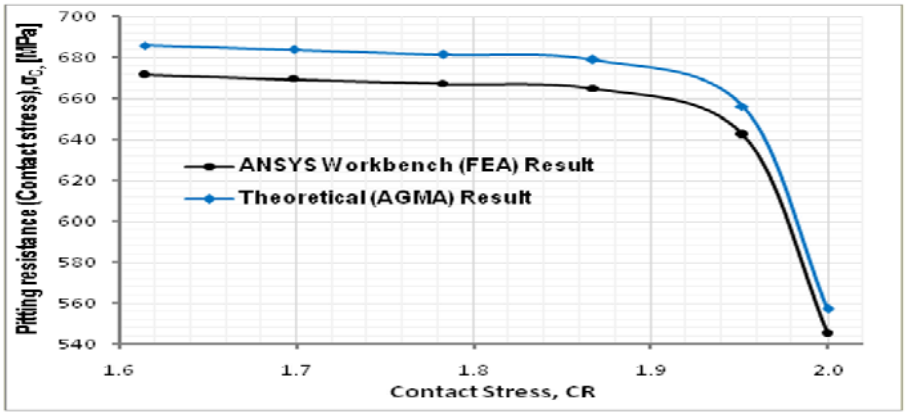

Figure 5.12: Pitting resistance (contact stress) versus contact ratio

Based on the contact stress results of ANSYS and AGMA equations the relations discussed below are analyzed. In figure (5.13a) the relation between stress cycle factor and contact ratio, then in figure (5.13b) the relation between number of load cycles and stress cycle factor. On figure (5.14) and figure (5.15) relation of safety factor and number of load cycles respectively with contact ratio are plotted.

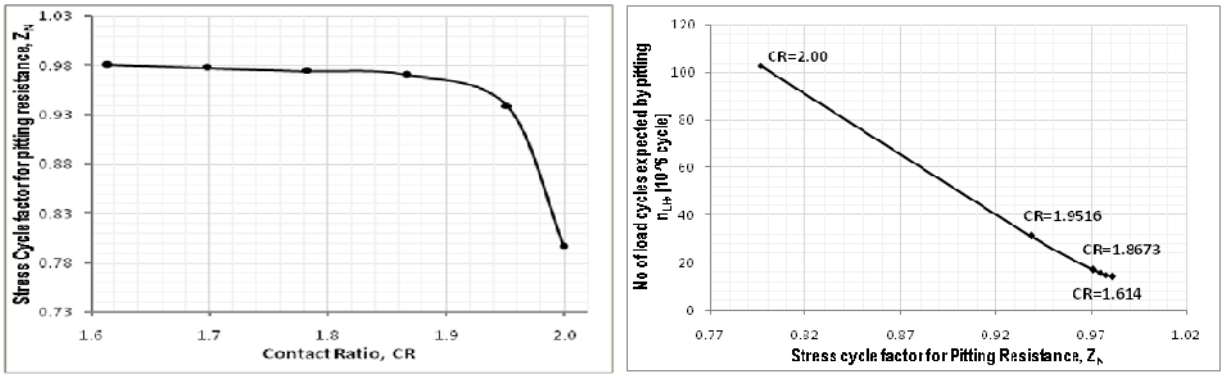

(a) (b)

Figure 5.13: Stress cycle factor for pitting resistance and number of load cycles: (a) Stress cycle factor versus contact ratio, (b) number of load cycles expected by pitting versus stress cycle factor for pitting

The stress cycle factor is calculated from equation (3.38). As the contact ratio increases the stress cycle factor value decreases as shown in figure (5.15). On the other hand the lower the stress cycle factor the higher fatigue life of the gear teeth will have. This shows that stress cycle factor is inversely proportional with the number of load cycles and safety factor, figure (5.13b).

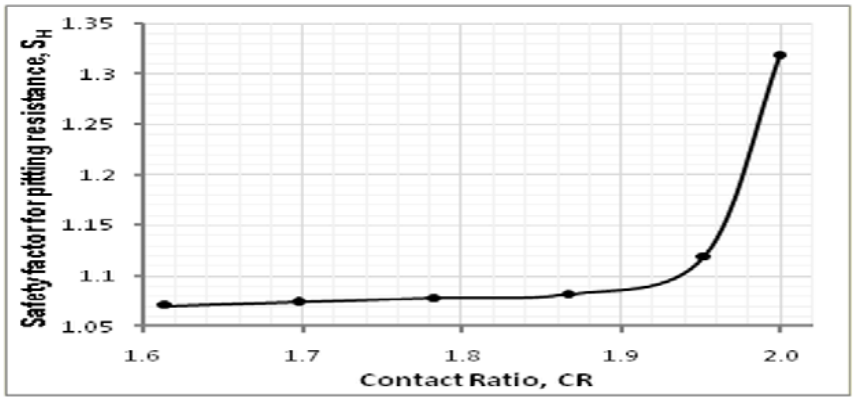

Figure 5.14: Safety factor for pitting resistance versus contact ratio

The relation of safety factor with the contact ratio is shown on the figure (5.14). The safety factor is directely proportional with the contact ratio. When the CR increases, the safety factor of the pinion tooth under mesh increases, for the same applied torque.

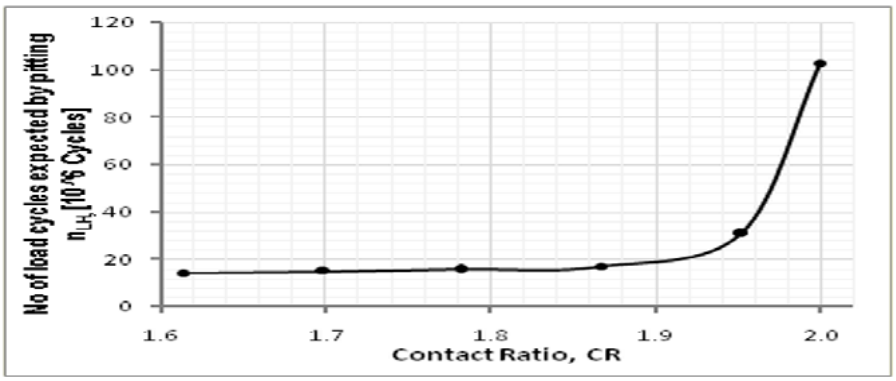

Figure 5.15: Number of load cycles expected by pitting versus contact ratio

The number of load cycles is determined from equation (3.40b). The number of cycles expected by the pitting resistance shows slight increase for the single pair of teeth contact, until the contact ratio comes to 1.90, on the other hand for contact ratio above 1.90 it shows large increase. This is because of the load sharing which is carried on the pair of teeth in mesh is similar at the higher point of single teeth contact

(HPSTC) for the ranges available until CR=1.90. however; since load sharing of the tooth under mesh becomes lower for the other conditions, (for the contact ratios above 1.90) the load cycle graph shows large increase, for instance for CR of 2.00 it reaches above 10^8 cycles while for those below 1.9 is not more than 2(10^7) cylcle.

5.6 Fatigue Sensitivity and Fatigue Life

This plot shows how the fatigue life results change as a function of the loading at the critical contact point for the six contact ratio gearing models. The result on figure (5.16) and (5.17) show the fatigue life for non constant loading (from 50% to 150% of the 25Nm applied torque). The graphs in figure (5.16) are directly obtained from ANSYS workbench analysis results where as the one in figure (5.17) is obtained from exel word (to show how they vary from each other) after extructing the results of ANSYS workbench (figures (5.16)).

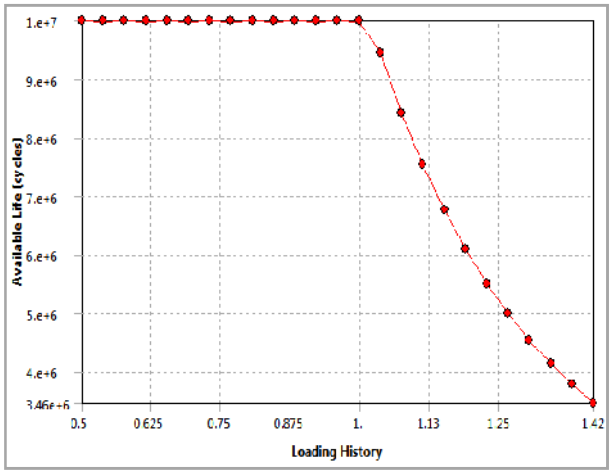

(a)

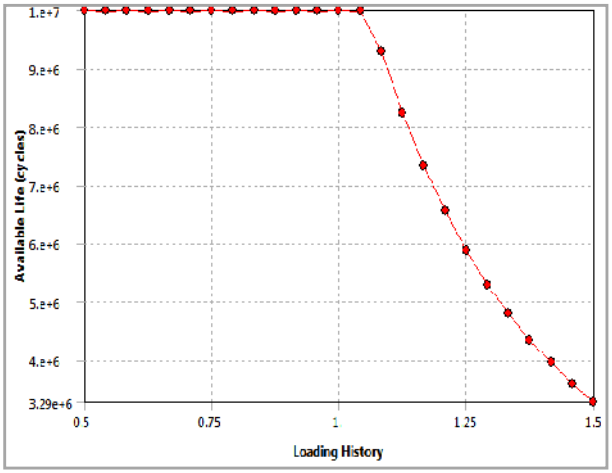

(b)

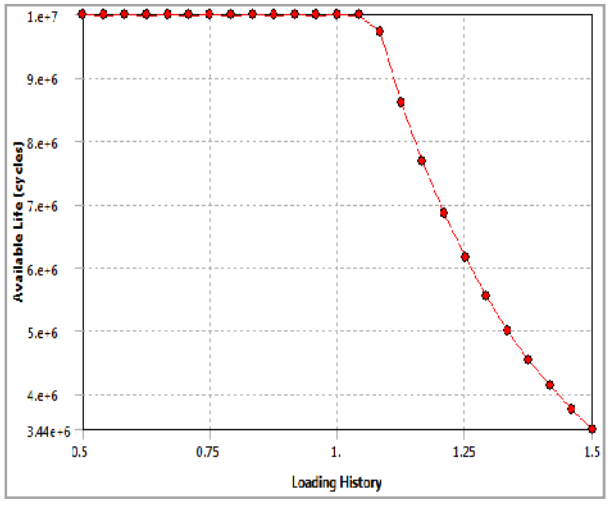

(c)

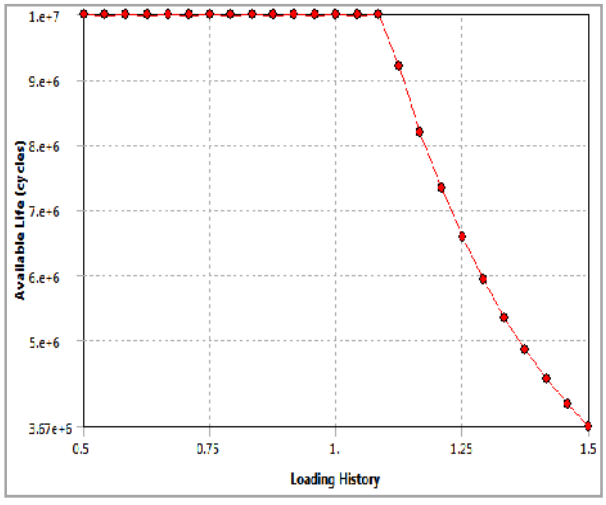

(d)

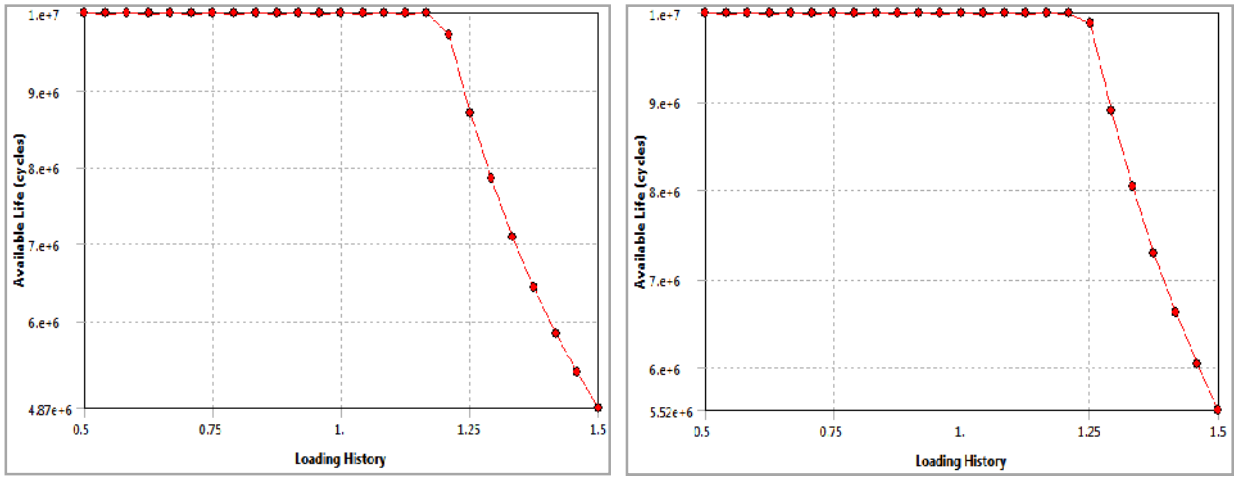

(e) (f)

Figure 5.16: fatigue sensitivity (available life cycles versus loading history): (a) for contact ratio = 1.614, (b) for contact ratio = 1.6985, (c) for CR = 1.7829, (d) for CR= 1.8673, (e) for CR = 1.9516, (f) for CR = 2.0

The contact sensitivity (the available fatigue life cycle for different loading (other than 25Nm)) of the six different gearing is plotted in figure (5.17).

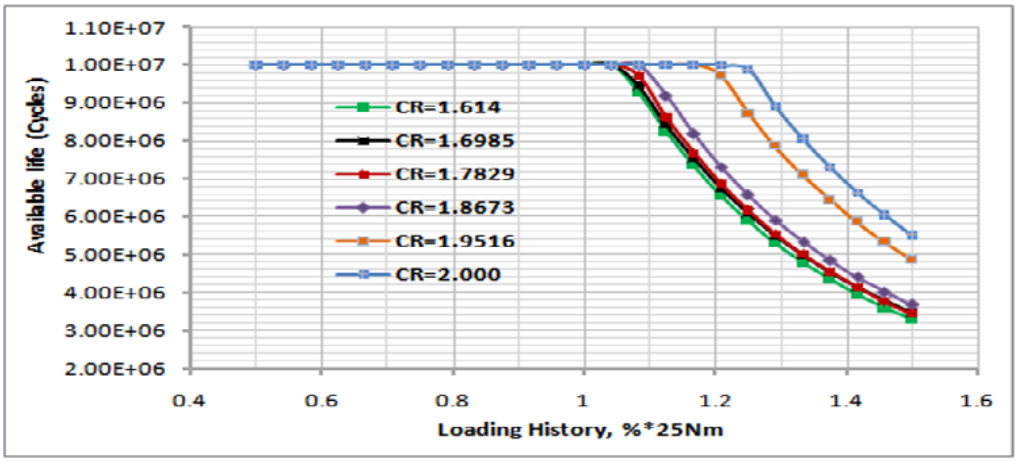

Figure 5.17: Path of Life cycle for six contact ratio gearing between 1.6 and 2.00 due to variable loading history

On the other hand, the contour plot represents the number of cycles at the critical contact point until the part will fail due to fatigue. Figure (5.18) shows contour plot of the fatigue life for each of the contact ratio gearing along the critical contact point. From the FEA requirement in a constant amplitude analysis, if the alternating stress is lower than the lowest alternating stress defined in the S-N curve, the life at that point is acceptable. Since the loading is proportional, the critical fatigue location can be determined by looking on the set of FEM results, figure (5.18).

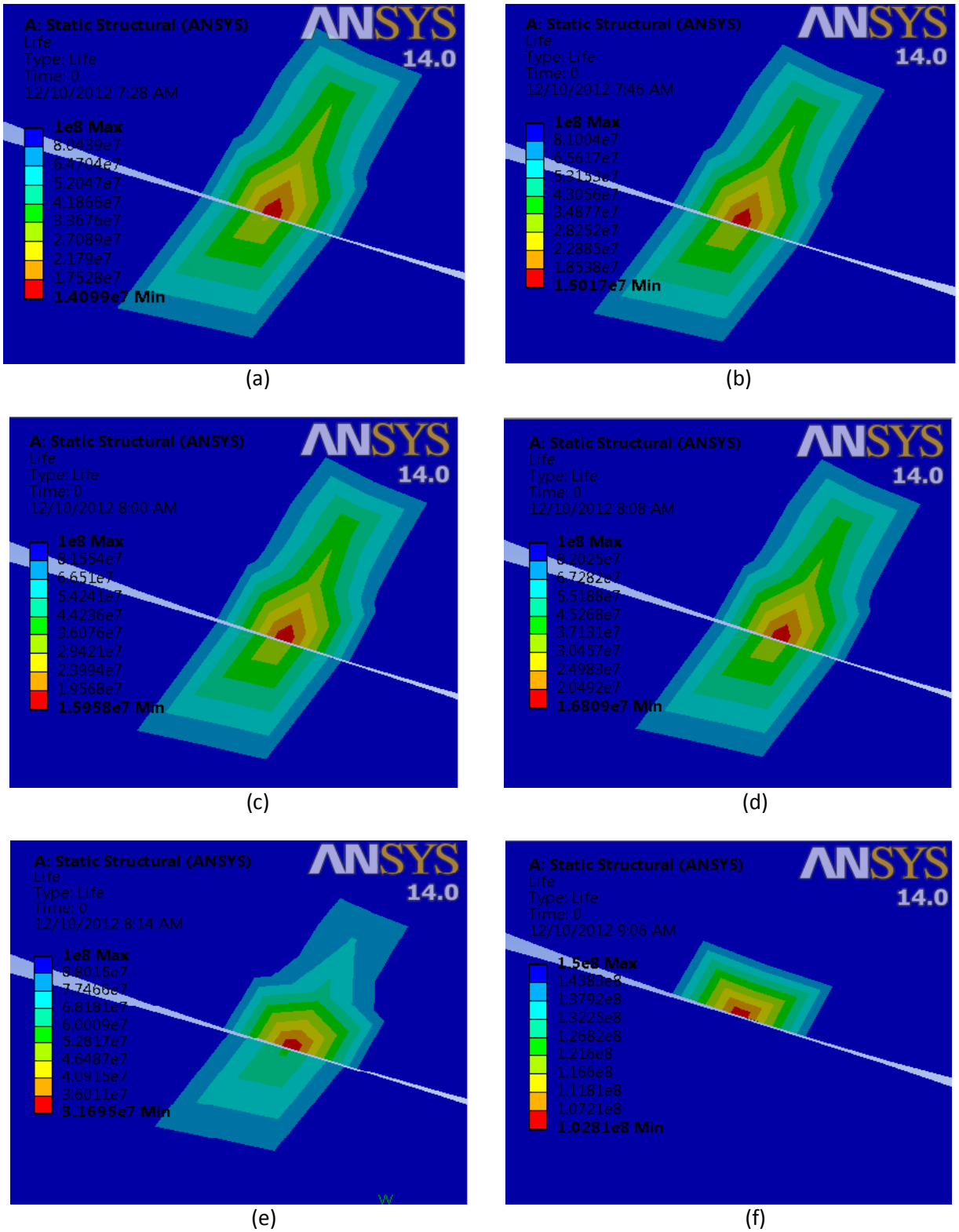

Figure 5.17: Number of fatigue life: (a) for contact ratio = 1.614, (b) for contact ratio = 1.6985, (c) for contact ratio = 1.7829, (d) for contact ratio= 1.8673, (e) for CR = 1.9516, (f) for CR = 2.0

In the present case, the higher the contact ratio will have the higher fatigue life before it comes to fail in contact stress. The fatigue life for each of the considered models is shown in the table (5.3) for the same applied torque, 25Nm.

Table 5.3: Number of fatigue life

Case No	Contact ratio	Stress cycle factor for pitting resistance, Z_N	No of fatigue life, n_{LH} [10^6cycles]
1	2.0	0.7964	102.81
2	1.9516	0.9384	31.695
3	1.8673	0.9708	16.809
4	1.7829	0.9743	15.958
5	1.6985	0.9778	15.017
6	1.614	0.9811	14.099

CHAPTER SIX

6 CONCLUSION AND RECOMMENDATION

In this thesis work, in order to make FEA analysis, 3D gear teeth modeling using CATIA is developed then to create the different contact positions Solid Works software is used, finaly to make the FEA analysis ANSYS Workbench is taken as a tool. Comparison of FEA result with analytical method is done. The AGMA and FEA calculations give comparable results for the contact stress (pitting resistance).

The stresses generated on spur gear teeth change with changing the contact ratio of gear. This is because of the change in value, location and direction of load applied on involute tooth in mesh to transmit power. The maximum percentage of load sharing occurs at the HPSTC line in the case of a normal contact ratio gearing, $CR < 2$. The maximum contact stresses generated at the critical load sharing position decreases with increasing the contact ratio. When the contact ratio is changed from (1.9) to (2.0), the decrease of stresses was more than the decrease of stresses when the contact ratio is changed between any two other successive cases. This is because that the critical load is 68% of the transmitted load when (C.R=2.0). As a result, failure in pitting of gear teeth is higher for lower contact ratio gearing. In other words, The higher the contact ratio of the spur gear is the higher the resistance for pitting. Higher contact ratio gearing is gained by modifying the addendum of spur gear teeth.

Finally, the obvious criteria for comparison among FEA and Analytical methods (AGMA) and experimental techniques, are accuracy, cost and time. Therefore since the result obtained from the FEA is comparable with the traditional one it is preferable to use FEA due to the vast capability in solving mechanical problems where ever AGMA does not have similar methods.

REFERENCES

1. A.P. Boresi and O.M. Sidebottom, ***Advanced Mechanics of Materials***, John Wiley & Sons, 1985
2. Ali R.H., ***Contact Stress Analysis of Spur Gear Teeth Pair***, World Academy of Science, Engineering and Technology, Tokyo, Japan, 2009
3. Andrew Sommer, Jim Meagher, Xi Wu, ***an Advanced Numerical Model of Gear Tooth Loading from Backlash and Profile Errors, 1998.***
4. ANSI/AGMA 2001-D04, ***Fundamental Rating Factors and Calculation Methods for Involute Spur and Helical Gear Teeth***, 2001
5. ANSI/AGMA Standard 2101-D04, ***Fundamental Rating Factors and Calculation Methods for Involute Spur and Helical Gear Teeth***, 2004
6. ANSYS (2009), ***Release 14.0, SAS IP, ANSYS Inc. U.S.A***., (www.ansys.com)
7. B.Venkatesh, V.Kamala and A.M.K.Prasad, ***Modeling and Analysis of Aluminum A360 Alloy Helical Gear for Marine***, international journal of applied engineering research, Volume 1, No 2, 2010
8. Colbourne J.R., ***the Geometry of Involute Gears***, Springer-Verlag, New York, 1987
9. Douglas Wright, ***Notes on Design and analysis of Machine element***, last updated May 2005
10. Durmus Gunay and Halil ÖZER, ***Effect of Rim Thickness on the Root Stresses of Spur Gear Tooth,*** Journal of Engineering Sciences, 1996
11. Elkholy,A.H., ***Tooth load sharing in high contact ratio spur gears***, Trans, ASME, Journal of Mechanisms, Transmission and Automation in Design, Vol.107, No.1, 1985
12. Evgeny Podzharov*, Vladimir Syromyatnikov and J. P. P. Navarro, ***Static and Dynamic Transmission Error in Spur Gears***, the Open Industrial and Manufacturing Engineering Journal, 2008
13. Faydor L. Litvin, ***Gear Geometry and Applied Theory***, 2nd ed., University of Illinois at Chicago, Cambridge University Press, New York, 2004
14. Fernandes, P. J. L., ***Engineering Failure Analysis***, 3(3), 219 225, 1996.
15. G. González Rey, R. J. García Martín, and P. Frechilla Fernández, ***Strength-Life Theory Can Help Avoid Gear Fatigue Failure***, 2007
16. G. Lundberg and A. Palmgren, ***Dynamic Capacity of Rolling Bearings***, Acta Polytech, Vol 1 (No. 3), 1947
17. G.M. Maitra., ***Handbook of Gear Design***. 2nd ed., McGraw-Hill Publishing: New Delhi, 1997
18. H. Hertz, ***Miscellaneous Papers by H. Hertz***, Jones & Schott, Macmillan, London, 1986
19. ISO 6336-1: ***Calculation of load capacity of spur and helical gears***. ISO, 1996
20. J. Shigley, ***Mechanical Engineering Design***, Eighth Edition, McGraw-Hill, USA, 2006
21. K. C. Ludema, ***Hand book of lubrication theory and practice of tribology***, CRC press, 1983
22. M. Rameshkumar, G. Venkatesan and P. Sivakumar, ***Finite Element Analysis of High Contact Ratio Gear***, AGMA Technical Paper, DRDO, Ministry of Defense, 2010
23. M. Rameshkumar, G. Venkatesan and P. Sivakumar, ***Finite Element Analysis of High Contact Ratio Gear***, American Gear Manufacturers Association technical resource, 2010
24. P. Kumar, ***Static and Dynamic Analysis of HCR Spur Gear Drive Using Finite Element Analysis***, MSc thsis, National Institute of Technology Rourkela, 2009
25. P.J.L. Fernandes and C.McDuling, ***Surface Contact Fatigue Failures in Gears***, Advanced Engineering and Testing Services, CSIR, South Africa, 1997

26. R.S. Khurmi, J.K. Gupta, ***a Textbook of Machine Design***. 14th ed. Eurasia Publishing House: Ram Nagar, New Delhi, 2005
27. Robert Basan*, Marina Franulovic* and Božidar Križan*, ***Numerical Model and Procedure for Determination of Stresses in Spur Gears Teeth Flanks***, Faculty of Engineering, University in Rijeka, SLOVAKI, 2008
28. Robert. L. Norton, ***Machine Design an integrated approach***. 3rd ed. Pearson prentice Hall: Upper Saddle River, 2006
29. Rubén D. Chacón; Luis J. Andueza; Miguel A. Díaz, ***Analysis Of Stress Due To Contact Between Spur Gears***, Advances in Computational Intelligence, Man-Machine Systems and Cybernetics, 2005
30. Sabah M.J. Ali, and Omar D. Mohammad, ***Load Sharing On Spur Gear Teeth And Stress Analysis When Contact Ratio Changed***, Al-Rafidain Engineering, 2007
31. Sabah M.J.Ali, and Omar D.Mohammad, ***Load Sharing on Spur Gear Teeth and Stress Analysis When Contact Ratio Changed***, College of Engineering \ University of Mosul, 2007
32. Shreyash Patel, ***Finite Element Analysis of Stresses in Involute Spur & Helical Gear***, MSc thesis, THE UNIVERSITY OF TEXAS AT ARLINGTON, 2010
33. Smith J. O. and Liu C. K., ***Stresses Due to Tangential and Normal Loads on Elastic Solid with Application to Some Contact Problems***, Journal of Applied Mechanics, Vol. 20, 1953
34. Solomon T., ***Finite Element Based Surface Fatigue Estimation in Involute Spur Gear under Rolling Sliding Contact Conditions***, MSc., thesis, Addis Ababa Institute of Technology, Addis Ababa, 2011
35. Sorin Cănănău, ***3d Contact Stress Analysis for Spur Gears***, University "POLITEHNICA" of Bucharest, Romania, 2003
36. Suzuki Y., ***Trend of Transmission and Gear Technology***, JSME preprint –mpt2004 symposium (in Japanese), No. 04-17, pp. 1-4.
37. T.E. Tallian, ***Failure Atlas for Hertz Contact***, ASME, 1992
38. Tuan Nguyen, ***Compact Design for Non-Standard Spur Gears***, journal of Mechanical, Aerospace and Industrial Engineering, Volume 2, Issue 1, 2011
39. Vanyo Kirov, ***Comparing AGMA and FEA Calculations***, 2011
40. Vitor Manuel, ***Investigations on Surface Damage by Rolling Contact Fatigue in Elastohydrodynamic Contacts Using Artificial Dents***, MSc thesis, Faculty of Engineering, University of Porto, 2005
41. Zeping Wei, ***Stresses And Deformations in Involute Spur Gears by Finite Element Method***, MSc. Thesis, University of Saskatchewan Saskatoon, Saskatchewan, 2004